



**NUS**  
National University  
of Singapore

# **Expanding the “minimalist” small molecule tagging approach to different classes of bioactive compounds**

A Thesis Submitted in Partial Fulfilment of the Requirements for Graduation with a  
Degree of Bachelor of Science (HONORS) from Department of Chemistry

By NIE Shikun

Supervisor: Prof. Dr. Yao Shao Qin

Mentor: Dr. Li Zhengqiu, Mr. Peng Bo

*Department of Chemistry, National University of Singapore,  
3 Science Drive 3, Singapore,  
117543, Singapore*

## Table of Contents

List of Figures, Schemes and Tables.....	II
Index of Abbreviations.....	III
1. Abstract.....	1
2. Introduction.....	1
2.1 Target identification and affinity-based probes.....	1
2.2 “Minimalist” linkers.....	3
2.3 The library of bioactive molecules.....	4
2.4 Project objectives and design.....	4
3. Experimental.....	7
3.1 General information.....	7
3.2 Linker synthesis.....	8
3.3 Probe synthesis.....	11
3.4 Structures of biotin-rhodamine azide and the negative probe .....	15
3.5 Cell culture and western blot.....	15
3.6 TNKS1/2 and bacterial lysate labelling with probe XA1.....	16
3.7 Cytotoxicity assay of the probe CA1 and wild-type camptothecin .....	17
3.8 <i>In vitro</i> and <i>in situ</i> proteome labelling in HepG2 cell lines.....	17
3.9 Target protein pull-down and western blotting.....	18
3.10 Cellular imaging.....	19
4. Results and Discussion.....	20
4.1 Linker synthesis scheme.....	20
4.2 Probe synthesis scheme.....	21
4.3 TNKS1/2 overexpression and purification.....	24
4.4 Enzymatic activity assay of XA1.....	25
4.5 <i>In vitro</i> TNKS2 and bacterial lysate labelling.....	26
4.6 <i>In vitro</i> and <i>in situ</i> HepG2 proteome labelling.....	28
4.7 Pull down and western blot.....	29
5. Conclusion.....	30
6. Future Work.....	30
7. Acknowledgements.....	31
8. References.....	31
Supporting Information.....	S1

## List of Figures, Schemes and Tables

<b>Figures</b>	<b>Page</b>
1. Illustration of ABP and A <sub>f</sub> BP approach	2
2. Illustration of one-step and two-step labelling	3
3. Structures of biotin-rhodamine azide and the negative probe	15
4. Mechanism of carboxyl activating by EDC	22
5. TNKS1 and TNKS2 purification	25
6. IC <sub>50</sub> measurement of XA1	26
7. TNKS1/2 labelling	27
8. Bacterial lysate labelling	28
9. <i>In vitro</i> and <i>in situ</i> proteome reactivity profiles in HepG2 cell lines	29
10. <i>In vitro</i> PD/WB for 4 of the probes FG1, EN1, NL1 and CA1	30

<b>Schemes</b>	<b>Page</b>
1. Synthetic route of “minimalist” linker L1-L3	20
2. Coupling scheme between the bioactive molecules and the “minimalist” linkers	22
3. Proposed coupling scheme between camptothecin and “minimalist” linkers	23

<b>Tables</b>	<b>Page</b>
1. Structures of the bioactive molecules and their corresponding probes	5

## Index of Abbreviations

ABPP	Activity based proteomic profiling
ABP	Activity based probe
AfBP	Affinity based probe
CDI	1,1'-Carbonyldiimidazole
DCC	<i>N,N'</i> -Dicyclohexylcarbodiimide
DCM	Dichloromethane
DMAP	4-Dimethylaminopyridine
DMF	<i>N,N</i> -Dimethyl formamide
DMSO	Dimethyl sulfoxide
EC <sub>50</sub>	Half maximal effective concentration
EDC	1-Ethyl-3-(3-dimethylaminopropyl)carbodiimide
HDAC	Histone deacetylase
HIF	Hypoxia inducible factor
IC <sub>50</sub>	Half maximal inhibitory concentration
IDO	Indoleamine-(2,3)-dioxygenase
KSP	Kinesin spindle protein
LAH	Lithium aluminium hydride
LCMS	Liquid chromatography mass spectrometer
LDA	Lithium diisopropylamine
PARP	Poly (ADP-ribose) polymerase
PD	Pull-down
PHD	Prolyl hydroxylase
PPAR	Peroxisome proliferator-activated receptor
TBTA	Tris[(1-benzyl-1 <i>H</i> -1,2,3-triazol-4-yl)methyl]amine
TCEP	Tris(2-carboxyethyl) phosphine
TEA	Triethylamine
TNKS	TRF1-interacting ankyrin-related ADP-ribose polymerase
UV	Ultraviolet
WB	Western Blot
WT	Wide type
XTT	2,3-Bis-(2-Methoxy-4-Nitro-5-Sulfophenyl)-2 <i>H</i> -Tetrazolium-5-carboxanilide

## 1. Abstract

“Minimalist” small molecule tagging approach<sup>1</sup> is promising in expanding the coverage of activity-based proteomic profiling (ABPP). Probes with “minimalist” incorporated are in general cell-permeable, clickable and preserve most of the biological activities from their parental bioactive molecules. In this project, several bioactive molecules, which target a range of protein classes, were installed with the “minimalist” linkers to generate the corresponding A/BPs. Subsequently these A/BPs were subjected to an array of biological experiments including enzymatic assay, XTT-based cytotoxicity assay, pure protein labelling, bacterial lysate labelling, mammalian proteome labelling, *in situ* pull-down conjugated with western blotting, and cellular imaging. The reported targets of these bioactive molecules were successfully pulled down, enriched and verified against specific antibodies. In conclusion, our extensive studies strongly suggest that the “minimalist” small molecule tagging approach readily expands the number of protein classes addressable by ABPP and facilitates the systematic analysis of their functions in human disease.

## 2. Introduction

### 2.1 Target identification and affinity-based probes

As organic synthesis advances and the strategy for natural product isolation improves, a myriad of bioactive molecules emerge at all times, however, majority of which the putative targets are unknown. Identification of the potential targets of these interesting molecules are imperative and crucial in drug discovery pipeline since the knowledge of the full spectrum of targets associated with a bioactive molecule enables a scientist to gain insights into biological processes, to understand the key pathways, to investigate the side effects and minimize the possible toxicity at an earlier stage. To date, instead of mechanism based profiling of enzymes<sup>2</sup>, activity-based proteomic profiling outstands as a general *in situ* approach for profiling small bioactive molecules<sup>3</sup>. In this method, the cell-permeable probe constructed from the corresponding small bioactive molecule is able to label active, but not inactive (e.g. inhibitor-bounded) target proteins in a matrix of complex proteome as well as to enrich target proteins for subsequent large-scale proteome-wide identification (e.g. LCMS/MS). These probes fall into two general categories, activity-based probes (ABPs) and affinity based probes

(A<sub>f</sub>BPs), of which the classification is based on distinguishable characteristics of ligand-protein interactions involving either covalent bonds or non-covalent bonds<sup>4,5</sup>.

### ABPs versus A<sub>f</sub>BPs

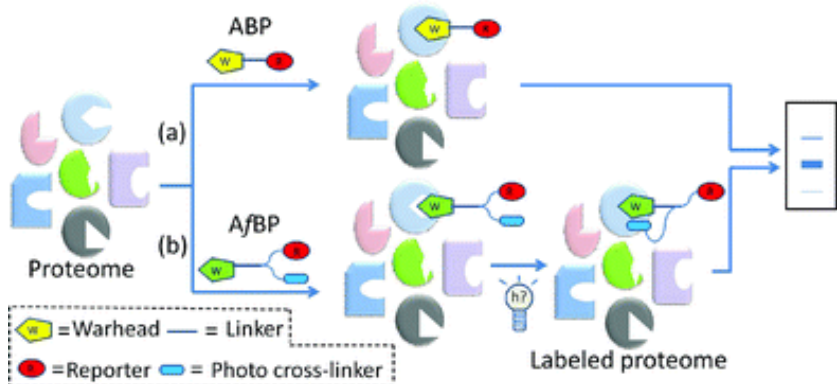


Figure 1: Illustration of ABP and A<sub>f</sub>BP approach<sup>4</sup>

A<sub>f</sub>BPs turn out more challenging in design. In brief, an A<sub>f</sub>BP is an ensemble of three essential modules, the core unit (a.k.a. the recognition unit), the linkage unit (a.k.a. the warhead unit for ABPs) and the reporter unit. The core unit is the corresponding bioactive molecule (e.g. inhibitor, agonist, or antagonist) that can bind to its putative proteins in cellular matrix. The linkage unit is a chemically stable, however reactive moiety that is able to covalently and irreversibly tether the target proteins. This unit is unique compared to ABPs since interaction between the core unit and its putative proteins is purely affinitive and non-covalent. Throughout the years, tremendous attentions have been paid to develop appropriate functionality and feasible mechanism for such a unit. Photoaffinity labelling technique has come to the fore in recent years<sup>6-8</sup> and has been first demonstrated for Dasatinib in 2012<sup>9</sup>, of which the probes contain a critical diazirine or benzophenone group. Upon UV irradiation, this diazirine or benzophenone generate a transient radical intermediate which could readily insert into proteins. The reporter unit is a non-native, however negligibly perturbing tag (e.g. fluorescent tags containing rhodamine moiety, affinity tags containing biotin) in one-step labelling or a ligation handle that can be bio-conjugated to an exogenously delivered tags in two-step labelling<sup>8</sup>.

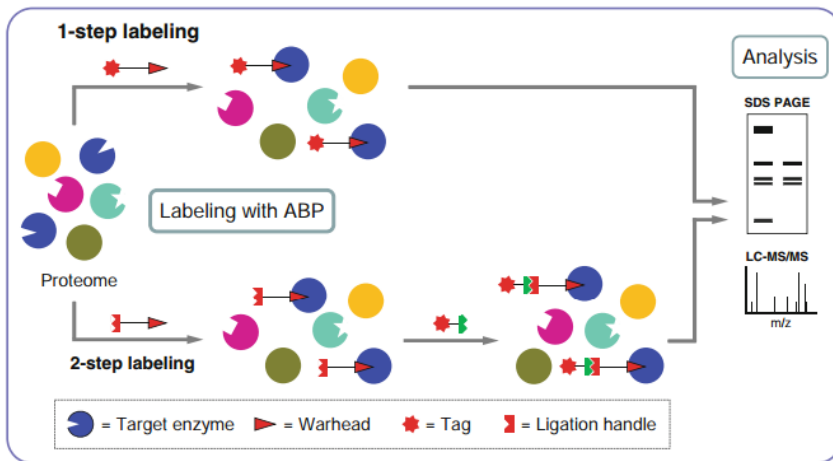


Figure 2: Illustration of one step and two step labelling<sup>8</sup>

## 2.2 “Minimalist” linkers

Though any additional modification on a bioactive molecule may affect its ideal biological activities, minimizing the modification size could probably alleviate this problem to some extent. The first-ever “minimalist” linkers containing the linkage and reporter unit, which could be easily incorporated into a bioactive molecule (i.e. the core unit) have been proposed by Dr. Li and his co-workers in 2013<sup>1</sup>. There are three versions all containing a diazirine photo-cross linkage unit and an alkyne handle, however of which one possesses an iodo substituent, one possesses a carboxylic group and the other one possesses an amine group (L1-L3 see scheme 1). These innovative molecules hold piles of brilliant chemical properties. Firstly, the advantage of diazirine photocrosslinker unit over aryl azide<sup>10</sup>, benzophenone<sup>11</sup> and other common photoreactive groups lies in its efficiency in absorption at a wavelength of 350-380nm, the range of which causes no significant damages to biological systems. Diazirine is also stable towards strongly basic, acidic, oxidizing or reducing agents. Secondly, compared to bulky reporter in one-step labelling, the alkyne ligation handle ensures a minimal structure and through click chemistry, exogenous fluorescent or affinity tags could be readily ligated on since the ligation reaction is based on well-established copper-catalysed alkyne azide cycloaddition<sup>12-14</sup>. Based on our experiences, the choice of the photocrosslinker and the alkyne handle is critical to keep the overall probe small (< 800 Da) and cell-permeable. Thirdly, the three functional groups are envisioned to cover all possible incorporation reactions between the linker and the core. Lastly, these minimalist linkers are easily synthesizable through less than 10 steps (see scheme 1).

In Li's work, several probes assembled from different kinase inhibitors with minimalist incorporations were demonstrated for efficient *in situ* proteome profiling. The potential of this non-directed and photoreactive "minimalist"-tagging method to expand proteome coverage of ABPP is promising, yet to be thoroughly validated.

### *2.3 The library of bioactive molecules*

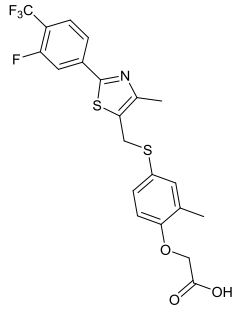
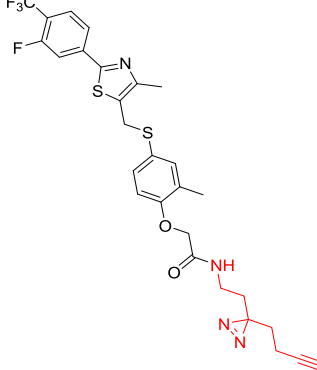
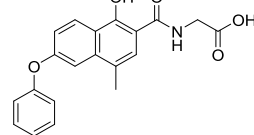
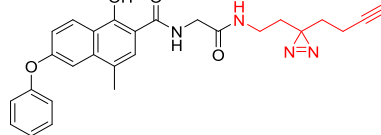
The innovation of minimalist linkers should greatly expand the number of protein classes addressable by ABPP. To demonstrate experimentally, a library of bioactive molecules that target diversified protein classes were chosen for incorporation with the "minimalist" linkers and the resulting probes were subsequently employed into various biological experiments. These molecules span a wide space of protein classes. Among the list, camptothecin is a plant alkaloid targeting DNA topoisomerase I, which displays nanomolar potency in cytotoxicity against many human cell lines, including HT29, LOX, SKOV3, and SKVLB, with IC<sub>50</sub> values ranging from 37 nM to 48 nM<sup>15</sup>. XAV-939 selectively inhibits Wnt/β-catenin-mediated transcription through tankyrase1/2 (TNKS1/2) inhibition with IC<sub>50</sub> of 11 nM/4 nM, and regulates axin levels however does not affect CRE, NF-κB or TGF-β<sup>16</sup>. FG-4592 is an oral inhibitor of hypoxia inducible factor (HIF) prolyl hydroxylase (PHD) currently in clinical development for the treatment of anaemia<sup>17</sup>. NLG919 is a potent indoleamine-(2,3)-dioxygenase (IDO) pathway inhibitor with K<sub>i</sub>/EC<sub>50</sub> of 7 nM/75 nM<sup>18</sup>. Entinostat strongly inhibits histone deacetylase 1 (HDAC1) and HDAC3 with IC<sub>50</sub> of 0.51 μM and 1.7 μM, compared with other HDACs 4, 6, 8, and 10<sup>19</sup>. Ispinesib is a potent, specific and reversible inhibitor of kinesin spindle protein (KSP) with K<sub>i app</sub> of 1.7 nM, however shows no inhibition to CENP-E, RabK6, MCAK, MKLP1, KHC or Kif1A<sup>20</sup>. GW0742 is a potent and highly selective peroxisome proliferator-activated receptor β/δ (PPARβ/δ) agonist, with IC<sub>50</sub> of 1 nM, 1000-fold selectivity over human PPARα and human PPARγ<sup>21</sup>.

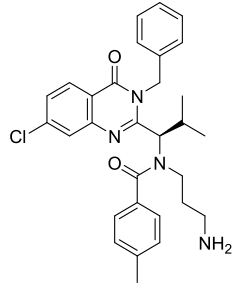
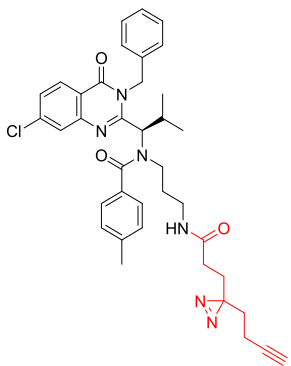
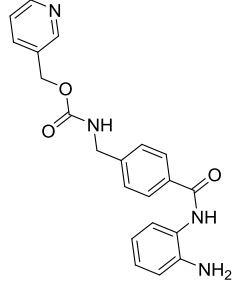
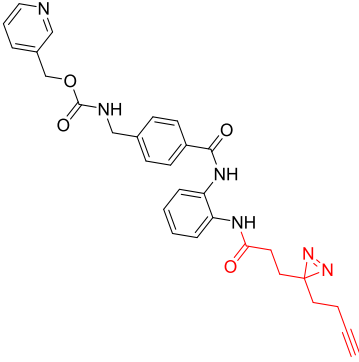
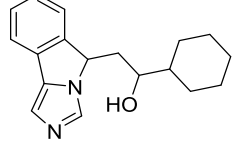
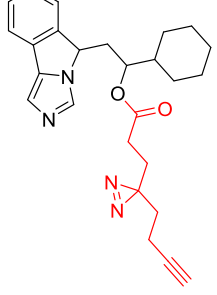
### *2.4 Project objectives and design*

In view of limited examples for the above "minimalist"-tagging strategy, this project aims to explore the potential application of such a promising strategy in ABPP and expand the proteome coverage of ABPP outside of kinase family. Diversified incorporation reactions are to be validated and constructed probes are to be utilized to interrogate putative targets in cellular matrix.

At first, a library of bioactive molecules were selected including nucleus or cytoplasm enzymes and agonists involved in different biological pathways. Next, the three versions of “minimalist” linkers were synthesized following the reported procedure<sup>1</sup>. These linkers were subsequently installed on several bioactive molecules to form the corresponding probes (see table 1). An array of biological experiments, including but not limited to pure protein labelling, bacterial lysate labelling, *in vitro* and *in situ* HepG2 proteome profiling, *in vitro* and *in situ* pull-down & western blotting, XTT cytotoxicity assay, enzymatic activity assay, were carried out to validate these AfBPs’ ability to label and enrich their putative proteins, however without appreciable deviation of biological activities from their parental bioactive molecules.

**Table 1:** Structures of the bioactive molecules and their corresponding probes. Linker incorporation sites were highlighted in red.

Structure of Bioactive Molecules	Structure of Probes	SAR references	Main Targets
 <b>GW0742</b>	 <b>GW1</b>	[21] <sup>21</sup>	PPAR $\beta/\delta$
 <b>FG-4592</b>	 <b>FG1</b>	[17] <sup>17</sup>	HIF2 $\alpha$ Hydroxylase (PHD1)

 <p><b>Ispinesib</b></p>	 <p><b>IS1</b></p>	<p>[20]<sup>20</sup></p>	<p>Kinesin Spindle Protein</p>
 <p><b>Entinostat</b></p>	 <p><b>EN1</b></p>	<p>[19]<sup>19</sup></p>	<p>Histone Deacetylase1/3 (HDAC1/3)</p>
 <p><b>NLG919</b></p>	 <p><b>NL1</b></p>	<p>[18]<sup>18</sup></p>	<p>Iondoleamine-(2,3)-dioxygenase (IDO)</p>

<p><b>Camptothecin</b></p>	<p><b>CA1</b></p>	<p>[15]<sup>15</sup></p>	<p>DNA Topoisomerase I (TOP1)</p>
<p><b>XAV-939</b></p>	<p><b>XA1</b></p>	<p>[16]<sup>16</sup></p>	<p>Tankyrase1/2 (TNKS1/2)</p>

### 3. Experimental

#### 3.1 General information

All chemicals were purchased from commercial vendors and used without further purification, unless indicated otherwise. All reactions requiring anhydrous conditions were carried out under argon or nitrogen gas using oven-dried glassware. HPLC-grade solvents were used for all reactions. Reaction progress was monitored by TLC on pre-coated silica plates (Merck 60 F254, 0.25 µm) and spots were revealed by UV lamp or iodine stain. Flash column chromatography was carried out using Merck 60 F254, 0.040-0.063 µm silica gel. Both <sup>1</sup>H-NMR and <sup>13</sup>C-NMR spectra were acquired on Bruker NMR spectrometers (either 300 MHz or 500 MHz for <sup>1</sup>H and either 75 MHz or 126 MHz for <sup>13</sup>C). Chemical shifts were expressed in parts per million referenced with respect to appropriate internal standards or residual solvent peaks (Proton CDCl<sub>3</sub> = 7.26 ppm, Carbon CDCl<sub>3</sub> = 77 ppm). The following abbreviations were used in reporting spectra, s = singlet, d = doublet, t = triplet, q = quartet, m = multiplet, dd = doublet of doublets, td = triplet of doublets. All analytical HPLC was carried out on a Shimadzu LCMS (IT-TOF) system. Water with 0.1% TFA and acetonitrile with 0.1%

TFA were used as eluents, the flow rate was 0.6 mL/min and elution time was 15 mins. All ESI-HRMS spectra were acquired on a Bruker MicrOTOF-Q II instrument. In enzyme inhibition and IC<sub>50</sub> measurement experiments, Tecan microplate reader (Multimode Reader, Infinite®200) in luminescence mode with i-control TM software was applied. Fluorescence scanning of the SDS-PAGE gels was carried out with Typhoon 9410 fluorescence gel scanner (Amersham Biosciences). Imaging was conducted with the Leica TCS SP5X confocal microscope system equipped with Leica HCX PL APO 63×/1.20 W CORR CS, 405 nm diode laser, white laser (470–670 nm, with 1 nm increments, with eight channels AOTF for simultaneous control of eight laser lines, each excitation wavelength provides 1.5 mV), and a photomultiplier tube (PMT) detector ranging from 410 to 700 nm for steady state fluorescence. Images were processed with Leica Application Suite Advanced Fluorescence (LAS AF). Antibodies against TNKS1, PPARδ, PHD1, TOP1, IDO and HDAC3 were purchased from Abcam. Plasmids carrying TNKS1/2 genes (catalytic domains with His tags) were provided by Johan Weigelt's group<sup>22</sup>. Wherever mentioned, the click master reagents were a freshly prepared equimolar mixture of either 5 mM tris[(1-benzyl-1H-1,2,3-triazol-4-yl)methyl]amine (TBTA) in DMSO, 50 mM aqueous tris(2-carboxyethyl) phosphine (TCEP), 50 mM aqueous CuSO<sub>4</sub> and 2.5 mM biotin-rhodamine azide in DMSO for pure protein, bacterial lysate and mammalian cell lysate labelling experiments, or 100 mM TBTA in DMSO, 1M aqueous TCEP, 1M aqueous CuSO<sub>4</sub> and 50 mM biotin-rhodamine azide in DMSO for pull-down western blot (PD-WB) experiments.

### 3.2 Linker synthesis

*Ethyl 3-oxohept-6-ynoate (I)* (serial number marked in scheme 1).

To a stirred solution of LDA, which was prepared freshly from diisopropylamine and *n*-butyl lithium in dry THF in -78°C acetone-dry ice bath, was added ethyl acetoacetate in 0°C ice bath. After 30 mins, propargyl bromide was added to the reaction mixture in one whole portion and the resulting mixture was stirred for 1h in ice bath, after which the reaction was quenched by drop-wise addition of water. The organic layer was extracted with ethyl acetate, washed with brine, dried over sodium sulphate, and finally evaporated off solvent by rotary evaporator to give the crude product. The crude product was purified by silica gel column using 10:1 hexane to ethyl acetate as mobile phase to give the purified eluent, which was evaporated off solvent by rotary evaporator

to give the colourless oil.  $^1\text{H}$  NMR (300 MHz,  $\text{CDCl}_3$ )  $\delta$  4.20 (q,  $J = 7.1$  Hz, 2H), 3.46 (s, 2H), 2.86 (t,  $J = 7.2$  Hz, 2H), 2.48 (td,  $J = 7.3, 2.6$  Hz, 2H), 1.96 (t,  $J = 2.6$  Hz, 1H), 1.28 (t,  $J = 7.1$  Hz, 3H).

*Ethyl 2-(but-3-yn-1-yl)-1,3-dioxolan-2-ylacetate (2).*

To a stirred solution of ethyl 3-oxohept-6-ynoate in benzene, ethylene glycol and *p*-toluenesulfonic acid were added sequentially. The resulting solution was refluxed for 6h, after which the reaction was quenched by water. The organic layer was extracted by ethyl acetate, washed by brine and dried over sodium sulphate to give crude product, which was purified by silica gel chromatography using 10:1 hexane to ethyl acetate as the mobile phase so as to give the pale yellow oil.  $^1\text{H}$  NMR (300 MHz,  $\text{CDCl}_3$ )  $\delta$  4.15 (q,  $J = 7.1$  Hz, 2H), 4.07 – 3.89 (m, 4H), 2.65 (s, 2H), 2.38 – 2.25 (m, 2H), 2.19 – 2.04 (m, 2H), 1.93 (t,  $J = 2.7$  Hz, 1H), 1.27 (t,  $J = 7.1$  Hz, 3H).

*2-(2-(but-3-yn-1-yl)-1,3-dioxolan-2-yl)ethan-1-ol (3).*

To a stirred suspension of lithium aluminium hydride in dry tetrahydrofuran at 0°C, ethyl 2-(2-(but-3-yn-1-yl)-1,3-dioxolan-2-yl)acetate was added drop-wise. After an additional stirring of 3h, the reaction was quenched by drop-wise addition of acetic acid. The resulting suspension was filtered under reduced pressure to give a clear solution, of which the organic layer was extracted by ethyl acetate, washed by brine and dried over sodium sulphate to give the crude product. The crude product was purified by 3:1 hexane to ethyl acetate to give eluent that upon solvent-evaporation resulted in the colourless oil.  $^1\text{H}$  NMR (500 MHz,  $\text{CDCl}_3$ )  $\delta$  4.07 – 3.79 (m, 4H), 3.69 (t,  $J = 5.7$  Hz, 2H), 2.76 (s, 1H), 2.36 – 2.09 (m, 2H), 2.01 – 1.74 (m, 5H).

*1-hydroxylhept-6-yn-3-one (4).*

To a stirred solution of 2-(2-(but-3-yn-2-yl)-1,3-dioxolan-2-yl)ethan-1-ol in acetone, was added *p*-toluenesulfonic acid. The reaction mixture was allowed to stir for an additional 2 h, followed by quenching with water. The organic layer was extracted by ethyl acetate, washed by brine and dried over sodium sulphate to give the crude product, which was purified by silica gel chromatography using 3:1 hexane to ethyl acetate to afford a pale yellow oil.  $^1\text{H}$  NMR (500 MHz,  $\text{CDCl}_3$ )  $\delta$  3.87 (t,  $J = 5.0$  Hz, 2H), 2.70 (m, 4H), 2.47 (t,  $J = 7.2$ , 2H), 2.35 (br, 1H), 1.96 (t,  $J = 2.7$  Hz, 1H). EI-MS: m/z calcd: 126.06; Found 126.09<sup>1</sup>.

*2-(3-(but-3-yl-1-yl)-3*H*-diazirin-3-yl)ethan-1-ol (5).*

Ammonia gas was condensed into a pressure-resistant vial that was immersed in acetone-dry ice bath. 1-hydroxylhept-6-yn-3-one was added to the stirred ammonia,

after which the vial was capped and the solution was stirred overnight. Hydroxylamine-*O*-sulfonic acid dissolved in methanol was added to the vial after the vial was cooled to -78°C. The resulting reaction mixture was stirred overnight without a stopper, after which the slurry was filtered with a mixture of methanol/water and the filtrate was extracted with dichloromethane. The organic layer was dried, evaporated off solvents to give light brown oil. Iodine powder was continuously added to the brown oil that was re-dissolved and stirred in dichloromethane at 0 °C until the reaction mixture turned dark red. The resulting solution was allowed to stir for half an hour, after which the ice bath was removed. After an additional stirring of 2 hours, the reaction mixture was quenched by sodium thiosulfate solution until it turned light orange. Extraction by dichloromethane followed by drying over sodium sulphate and *vacuo* evaporation afforded the crude product, which was purified by silica gel chromatography using 10:1 hexane to ethyl acetate to give the colourless oil. <sup>1</sup>H NMR (500 MHz, CDCl<sub>3</sub>) δ 3.51 (t, J = 8.2 Hz, 2H), 2.07 (m, 3H), 1.70 (m, 5H). EI-MS: m/z calcd: 138.07; Found 138.12<sup>1</sup>.

*3-(but-3-yn-1-yl)-3-(2-iodoethyl)-3H-diazirine (L3).*

Iodine powder was added to a stirred solution of triphenylphosphine and imidazole in dichloromethane at 0°C. The resulting solution was allowed to stir for 10min, after which 2-(3-(but-3-yl-1-yl)-3H-diazirin-3-yl)ethan-1-ol was added. The resulting solution was stirred overnight, after which it was quenched by addition of sodium thiosulfate at 0°C. The organic layer was extracted with dichloromethane, dried over sodium sulphate and evaporated off solvents in *vacuo* to afford the colorless oil. <sup>1</sup>H NMR (500 MHz, CDCl<sub>3</sub>) δ 2.89 (t, J = 7.5, 2H), 2.12 (t, J = 7.5, 2H), 1.98 (m, 3H), 1.70 (t, J = 7.3, 2H). EI-MS: m/z calcd: 247.98; Found 247.91<sup>1</sup>.

*3-(2-azidoethyl)-3-(but-3-yn-1-yl)-3H-diazirine (6).*

To a stirred solution of 3-(but-3-yn-1-yl)-3-(2-iodoethyl)-3H-diazirine in DMF, sodium azide was added. The resulting solution was allowed to stir overnight followed by quenching with water. The organic layer was extracted with ethyl acetate, dried over sodium sulphate and evaporated off solvents to afford the crude products, after which the crude products were purified via silica gel chromatography using hexane to ethyl acetate 10:1 as the mobile phase to give the light orange oil. <sup>1</sup>H NMR (500 MHz, CDCl<sub>3</sub>) δ 3.16 (t, J = 6.8 Hz, 2H), 2.08 – 1.97 (m, 3H), 1.76 – 1.63 (m, 4H). EI-MS: m/z calcd: 163.08; Found 163.05<sup>1</sup>.

*2-(3-(but-3-yn-1-yl)-3H-diazirin-3-yl)ethan-1-amine (L2).*

To a stirred solution of 3-(2-azidoethyl)-3-(but-3-yn-1-yl)-3H-diazirine in a mixture of 10:1 tetrahydrofuran and water was added triphenylphosphine. The resulting solution was stirred overnight, after which it was quenched by adding 1M HCl solution. The aqueous layer was washed by ethyl acetate, alkalized by 1M NaOH solution and extracted with ethyl acetate to give the organic layer, which was evaporated off solvents to afford the product.  $^1\text{H}$  NMR (300 MHz,  $\text{CDCl}_3$ )  $\delta$  2.51 (t,  $J = 6.9$  Hz, 2H), 2.09 – 1.94 (m, 3H), 1.74 – 1.56 (m, 4H), 1.45 (s, 2H). EI-MS: m/z calcd: 137.09; Found 137.13<sup>1</sup>.

*3-(3-(but-3-yn-1-yl)-3H-diazirin-3-yl)propanenitrile (7).*

To a stirred solution of 3-(but-3-yn-1-yl)-3-(2-iodoethyl)-3H-diazirine in DMF, potassium cyanide was added. The resulting solution was allowed to stir overnight followed by quenching with water. The organic layer was extracted with ethyl acetate, dried over sodium sulphate and evaporated off solvents to afford the crude products, after which the crude products were purified via silica gel chromatography using hexane to ethyl acetate 10:1 as the mobile phase to give the light orange oil.  $^1\text{H}$  NMR (300 MHz,  $\text{CDCl}_3$ )  $\delta$  2.19 (t,  $J = 7.6$  Hz, 2H), 2.09 – 2.00 (m, 3H), 1.87 (t,  $J = 7.6$  Hz, 2H), 1.70 (t,  $J = 7.0$  Hz, 2H). EI-MS: m/z calcd: 147.07; Found 147.12<sup>1</sup>.

*3-(3-(but-3-yn-1-yl)-3H-diazirin-3-yl)propanoic acid (**L1**).*

3-(3-(but-3-yn-1-yl)-3H-diazirin-3-yl)propanenitrile dissolved in 5mL 10% NaOH and 1mL methanol was refluxed at 80 °C for 7h, after which methanol was evaporated and the aqueous layer was washed by hexane. Following neutralization of the aqueous layer by 4M HCl, organic layer was extracted by ethyl acetate three times, washed by sodium chloride solution, dried over sodium sulphate and evaporated off solvents to afford the product.  $^1\text{H}$  NMR (500 MHz,  $\text{CDCl}_3$ )  $\delta$  2.18 (t,  $J = 7.7$  Hz, 2H), 2.05 – 1.96 (m, 3H), 1.82 (t,  $J = 7.6$  Hz, 2H), 1.66 (t,  $J = 7.4$  Hz, 2H).  $^{13}\text{C}$  NMR (75 MHz,  $\text{CDCl}_3$ )  $\delta$  206.36 (s), 82.53 (s), 69.30 (s), 32.19 (s), 28.00 (s), 27.75 (s), 27.44 (s), 13.22 (s). EI-MS: m/z calcd: 166.07; Found 166.01<sup>1</sup>.

### 3.3 Probe synthesis

*N-(2-(3-(but-3-yn-1-yl)-3H-diazirin-3-yl)ethyl)-2-(((2-(3-fluoro-4-(trifluoromethyl)phenyl)-4-methylthiazol-5-yl)methyl)thio)-2-methylphenoxy)acetamide (**GW1**)*

To a stirred solution of **GW0742** (5.0 mg, 0.01 mmol) in DMF, EDC (3.3 mg, 0.021 mmol), TEA (1.9 mg, 0.013 mmol) and **L2** (1.7 mg, 0.013 mmol) were added. The resulting solution was allowed to stir overnight, after which the reaction was quenched

by water and the organic layer was extracted by ethyl acetate (EA). The crude was purified by flash silica gel chromatography using 3:1 hexane/EA as running solvent so as to give a pale yellow compound (5.3 mg, 0.0090 mmol, 85%). <sup>1</sup>H NMR (500 MHz, CDCl<sub>3</sub>) δ 7.76 – 7.67 (m, 2H), 7.63 (t, J = 7.6 Hz, 1H), 7.20 (dd, J = 11.5, 3.2 Hz, 2H), 6.70 (d, J = 8.3 Hz, 1H), 6.62 (s, 1H), 4.47 (s, 2H), 4.13 (s, 2H), 3.22 (q, J = 6.4 Hz, 2H), 2.29 (s, 3H), 2.22 (s, 3H), 2.00 (td, J = 7.2, 2.6 Hz, 2H), 1.96 (t, J = 2.6 Hz, 1H), 1.77 (t, J = 6.6 Hz, 2H), 1.64 (t, J = 7.3 Hz, 2H). <sup>13</sup>C NMR (75 MHz, CDCl<sub>3</sub>) δ 167.95 (s), 155.52 (s), 151.62 (s), 135.94 (s), 132.22 (s), 131.48 (s), 127.67 (s), 125.97 (s), 121.55 (s), 114.35 (s), 114.05 (s), 111.95 (s), 82.47 (s), 69.43 (s), 67.41 (s), 33.92 (s), 33.92 (s), 32.43 (s), 32.26 (s), 32.14 (s), 29.69 (s), 26.74 (s), 16.33 (s), 14.88 (s), 13.15 (s). LCMS: m/z [M+H]<sup>+</sup>, calcd: 591.15, found: 591.0794. ESI-HRMS: m/z [M+H]<sup>+</sup>, calcd: 591.1506, found: 591.1507.

*N*-(2-((2-(3-(but-3-yn-1-yl)-3*H*-diazirin-3-yl)ethyl)amino)-2-oxoethyl)-1-hydroxy-4-methyl-6-phenoxy-2-naphthamide (**FG1**)

To a stirred solution of **FG-4592** (5.0 mg, 0.014 mmol) in DMF, EDC (3.3 mg, 0.021 mmol), DIEA (2.2 mg, 0.017 mmol) and **L2** (1.7 mg, 0.013 mmol) were added. The resulting solution was allowed to stir overnight, after which the reaction was quenched by water and the organic layer was extracted by EA. The crude was purified by flash silica gel chromatography using 2:1 hexane/EA as running solvent so as to give a pale yellow compound (5.2 mg, 0.0090 mmol, 79%). <sup>1</sup>H NMR (300 MHz, CDCl<sub>3</sub>) δ 12.55 (s, 1H), 8.60 (s, 1H), 8.36 (d, J = 9.4 Hz, 1H), 7.51 – 7.37 (m, 4H), 7.22 (t, J = 7.4 Hz, 1H), 7.16 – 7.07 (m, 2H), 6.32 (s, 1H), 4.16 (d, J = 6.2 Hz, 2H), 3.17 (q, J = 6.6 Hz, 2H), 2.69 (s, 3H), 2.04 – 1.95 (m, 3H), 1.72 (t, J = 6.7 Hz, 2H), 1.68 – 1.61 (m, 3H). <sup>13</sup>C NMR (75 MHz, CDCl<sub>3</sub>) δ 170.65 (s), 168.76 (s), 158.61 (s), 155.95 (s), 153.84 (s), 147.20 (s), 132.27 (s), 130.15 (s), 125.66 (s), 124.50 (s), 124.17 (s), 122.34 (s), 119.70 (s), 119.34 (s), 111.78 (s), 82.68 (s), 77.21 (s), 69.40 (s), 43.16 (s), 34.42 (s), 32.48 (s), 32.11 (s), 26.69 (s), 21.73 (s), 13.17 (s). LCMS: m/z [M+H]<sup>+</sup>, calcd: 472.20, found: 472.1967. ESI-HRMS: m/z [M+Na]<sup>+</sup>, calcd: 494.1799, found: 494.1811.

(*S*)-4-ethyl-3,14-dioxo-3,4,12,14-tetrahydro-1*H*-pyrano[3',4':6,7]indolizino[1,2-*b*]quinolin-4-yl 3-(3-(but-3-yn-1-yl)-3*H*-diazirin-3-yl)propanoate (**CA1**)

To a stirred solution of **L1** (2.9 mg, 0.017 mmol) in DMF at 0°C, EDC (4.5 mg, 0.029 mmol), DMAP (0.18 mg, 0.0014 mmol) were added. After 10min **Camptothecin** (5 mg, 0.014 mmol) was added. The resulting solution was allowed to stir overnight, after

which the reaction was quenched by water and the organic layer was extracted by EA. The crude was purified by flash silica gel chromatography using 95:5 DCM/methanol as running solvent so as to give a colourless compound (3.9 mg, 0.0079 mmol, 55%).  $^1\text{H}$  NMR (300 MHz,  $\text{CDCl}_3$ )  $\delta$  8.40 (s, 1H), 8.22 (d,  $J = 8.5$  Hz, 1H), 7.94 (d,  $J = 8.1$  Hz, 1H), 7.84 (t,  $J = 7.7$  Hz, 1H), 7.67 (t,  $J = 7.5$  Hz, 1H), 7.23 (s, 1H), 5.54 (dd,  $J = 85.8, 17.3$  Hz, 2H), 5.29 (s, 2H), 2.52 – 2.07 (m, 4H), 2.07 – 1.91 (m, 3H), 1.81 (t,  $J = 7.7$  Hz, 2H), 1.63 (t, 2H), 0.98 (t,  $J = 7.5$  Hz, 3H).  $^{13}\text{C}$  NMR (126 MHz,  $\text{CDCl}_3$ )  $\delta$  171.13 (s), 167.34 (s), 157.34 (s), 152.32 (s), 148.88 (s), 146.31 (s), 145.75 (s), 131.17 (s), 130.69 (s), 129.62 (s), 128.45 (s), 128.19 (s), 128.06 (s), 120.18 (s), 95.95 (s), 82.55 (s), 76.19 (s), 69.36 (s), 67.08 (s), 49.94 (s), 32.11 (s), 31.77 (s), 28.11 (s), 27.78 (s), 27.38 (s), 13.25 (s), 7.56 (s), 0.99 (s). LCMS:  $m/z$  [M+H] $^+$ , calcd: 497.18, found: 497.1798. ESI-HRMS: [M+Na] $^+$ , calcd: 519.1639, found: 519.1636.

*4-(2-(3-(but-3-yn-1-yl)-3*H*-diazirin-3-yl)ethoxy)-2-(4-(trifluoromethyl)phenyl)-7,8-dihydro-5*H*-thiopyrano[4,3-*d*]pyrimidine (**XAI**)*

To a stirred solution of **XAV-939** (5.0 mg, 0.016 mmol) in DMF,  $\text{K}_2\text{CO}_3$  (2.7 mg, 0.019 mmol) and **L3** (4.8 mg, 0.019 mmol) were added. The resulting solution was allowed to stir overnight, after which the reaction was quenched by water and the organic layer was extracted by EA. The crude was purified by flash silica gel chromatography using 20:1 hexane/EA as running solvent so as to give a pale yellow compound (5.8 mg, 0.013 mmol, 84%).  $^1\text{H}$  NMR (300 MHz,  $\text{CDCl}_3$ )  $\delta$  8.48 (d,  $J = 8.5$  Hz, 2H), 7.70 (d,  $J = 8.6$  Hz, 2H), 4.42 (t,  $J = 6.2$  Hz, 2H), 3.79 (s, 2H), 3.20 (t,  $J = 6.0$  Hz, 2H), 2.98 (t,  $J = 6.0$  Hz, 2H), 2.07 (td,  $J = 7.3, 2.3$  Hz, 2H), 1.98 (dd,  $J = 7.7, 4.6$  Hz, 3H), 1.75 (t,  $J = 7.4$  Hz, 2H).  $^{13}\text{C}$  NMR (75 MHz,  $\text{CDCl}_3$ )  $\delta$  165.75 (s), 164.61 (s), 159.57 (s), 140.77 (s), 128.25 (s), 125.33 (s), 113.46 (s), 82.52 (s), 77.20 (s), 69.39 (s), 61.39 (s), 33.49 (s), 32.41 (s), 26.52 (s), 25.34 (s), 23.12 (s), 13.28 (s). LCMS:  $m/z$  [M+H] $^+$ , calcd: 433.13, found: 433.1297. ESI-HRMS:  $m/z$  [M+H] $^+$ , calcd: 433.1304, found: 433.1310.

*1-cyclohexyl-2-(5*H*-imidazo[5,1-*a*]isoindol-5-yl)ethyl 3-(3-(but-3-yn-1-yl)-3*H*-diazirin-3-yl)propanoate (**NL1**)*

To a stirred solution of **L1** (3.5 mg, 0.021 mmol) in DCM at 0°C, EDC (4.5 mg, 0.035 mmol), DMAP (0.18 mg, 0.0021 mmol) were added. After 10min **NLG919** (5 mg, 0.018 mmol) was added. The resulting solution was allowed to stir overnight, after which the reaction was quenched by water and the organic layer was extracted by EA. The crude was purified by flash silica gel chromatography using 95:5 DCM/methanol as running solvent so as to give a colourless compound (3.7 mg, 0.0087 mmol, 49%).

<sup>1</sup>H NMR (300 MHz, CDCl<sub>3</sub>) δ 7.71 (s, 1H), 7.53 (d, *J* = 8.0 Hz, 2H), 7.37 (t, *J* = 7.7 Hz, 1H), 7.31 – 7.22 (m, 1H), 7.19 (s, 1H), 5.16 (dd, *J* = 8.1, 3.7 Hz, 1H), 5.01 – 4.89 (m, 1H), 2.50 – 2.30 (m, 1H), 2.22 – 2.06 (m, 1H), 2.07 – 1.54 (m, 19H), 1.47 (s, 1H). <sup>13</sup>C NMR (75 MHz, CDCl<sub>3</sub>) δ 171.49 (s), 144.20 (s), 128.49 (s), 126.40 (s), 123.92 (s), 120.14 (s), 82.46 (s), 77.14 (s), 73.66 (s), 69.19 (s), 57.55 (s), 41.98 (s), 37.27 (s), 32.18 (s), 28.43 (s), 28.11 (s), 27.84 (s), 27.69 (s), 27.46 (s), 26.11 (s), 25.80 (s), 13.17 (s). LCMS: *m/z* [M+H]<sup>+</sup>, calcd: 431.24, found: 431.2225. ESI-HRMS: *m/z* [M+H]<sup>+</sup>, calcd: 431.2442, found: 431.2456.

(*R*)-*N*-(1-(3-benzyl-7-chloro-4-oxo-3,4-dihydroquinazolin-2-yl)-2-methylpropyl)-*N*-(3-(3-(but-3-yn-1-yl)-3*H*-diazirin-3-yl)propanamido)propyl)-4-methylbenzamide (**IS1**)

To a stirred solution of **L2** (5.0 mg, 0.0097 mmol) in DMF, EDC (3.0 mg, 0.019 mmol), DIEA (1.5 mg, 0.012 mmol) and **Ispinesib** (5.0 mg, 0.0097 mmol) were added. The resulting solution was allowed to stir overnight, after which the reaction was quenched by water and the organic layer was extracted by EA. The crude was purified by flash silica gel chromatography using 3:1 hexane/EA as running solvent so as to give a pale yellow compound (5.1 mg, 0.077 mmol, 80%). <sup>1</sup>H NMR (500 MHz, CDCl<sub>3</sub>) δ 8.33 (d, *J* = 8.5 Hz, 1H), 7.69 (d, *J* = 1.8 Hz, 1H), 7.53 – 7.46 (m, 1H), 7.39 (d, *J* = 7.3 Hz, 3H), 7.32 (t, *J* = 7.4 Hz, 3H), 7.25 – 7.19 (m, 3H), 6.12 (d, *J* = 15.8 Hz, 1H), 5.70 (d, *J* = 10.5 Hz, 1H), 5.20 (d, *J* = 15.8 Hz, 1H), 4.49 (s, 1H), 3.53 – 3.29 (m, 2H), 2.95 (d, *J* = 12.4 Hz, 1H), 2.89 – 2.77 (m, 1H), 2.78 – 2.63 (m, 2H), 2.41 (s, 3H), 2.08 – 1.92 (m, 4H), 1.88 – 1.77 (m, 2H), 1.74 (t, *J* = 7.5 Hz, 2H), 1.59 (dd, *J* = 14.1, 6.9 Hz, 2H), 0.95 (d, *J* = 6.7 Hz, 3H), 0.37 (d, *J* = 6.3 Hz, 3H). <sup>13</sup>C NMR (126 MHz, CDCl<sub>3</sub>) δ 172.87 (s), 170.77 (s), 162.12 (s), 155.95 (s), 147.56 (s), 140.88 (s), 139.68 (s), 136.73 (s), 133.83 (s), 129.26 (s), 128.97 (s), 128.75 (d, *J* = 3.6 Hz), 128.17 (s), 127.70 (s), 127.23 (s), 126.80 (s), 126.10 (s), 82.61 (s), 69.20 (s), 59.56 (s), 45.52 (s), 41.82 (s), 36.58 (s), 32.43 (s), 30.28 (s), 30.01 (s), 28.87 (s), 28.02 (s), 27.72 (s), 21.38 (s), 19.14 (s), 18.29 (s), 13.25 (s). LCMS: *m/z* [M+H]<sup>+</sup>, calcd: 665.30, found: 665.2917. ESI-HRMS: *m/z* [M+Na]<sup>+</sup>, calcd: 687.2840, found: 687.2821.

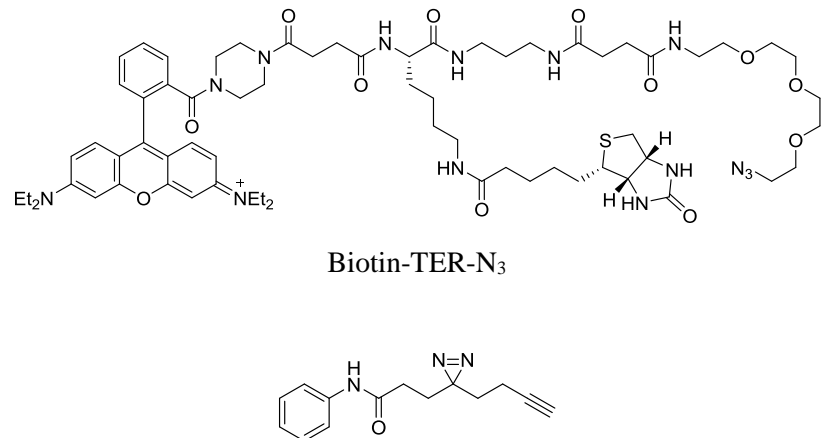
*pyridin-3-ylmethyl(4-((2-(3-(but-3-yn-1-yl)-3*H*-diazirin-3-yl) propanamido) phenyl) carbamoyl)benzyl)carbamate (**EN1**)*

To a stirred solution of **L2** (2.6 mg, 0.016 mmol) in DMF, EDC (4.1 mg, 0.027 mmol), DIEA (2.1 mg, 0.016 mmol) and **Entostat** (5.0 mg, 0.013 mmol) were added. The resulting solution was allowed to stir overnight, after which the reaction was quenched

by water and the organic layer was extracted by EA. The crude was purified by flash silica gel chromatography using 1:1 hexane/EA as running solvent so as to give a pale yellow compound (5.6 mg, 0.011 mmol, 81%).  $^1\text{H}$  NMR (500 MHz,  $\text{CDCl}_3$ )  $\delta$  9.16 (s, 1H), 8.61 (d,  $J = 24.0$  Hz, 2H), 8.36 (s, 1H), 7.90 (d,  $J = 7.9$  Hz, 2H), 7.74 (d,  $J = 7.6$  Hz, 1H), 7.58 (d,  $J = 7.9$  Hz, 1H), 7.40 (d,  $J = 7.9$  Hz, 2H), 7.36 – 7.31 (m, 1H), 7.19 (t,  $J = 7.4$  Hz, 2H), 7.09 (t,  $J = 7.9$  Hz, 1H), 5.39 (s, 1H), 5.18 (s, 2H), 4.47 (d,  $J = 5.9$  Hz, 2H), 2.09 (t,  $J = 7.5$  Hz, 2H), 1.98 (t,  $J = 2.5$  Hz, 1H), 1.94 (td,  $J = 7.4, 2.6$  Hz, 2H), 1.85 (t,  $J = 7.5$  Hz, 2H), 1.61 (t,  $J = 7.4$  Hz, 3H).  $^{13}\text{C}$  NMR (75 MHz,  $\text{CDCl}_3$ )  $\delta$  167.95 (s), 155.52 (s), 151.62 (s), 135.94 (s), 132.22 (s), 131.48 (s), 127.67 (s), 125.97 (s), 121.55 (s), 114.35 (s), 114.05 (s), 111.95 (s), 82.47 (s), 77.21 (s), 69.43 (s), 67.41 (s), 33.92 (s), 32.43 (s), 32.26 (s), 32.14 (s), 29.69 (s), 26.74 (s), 16.33 (s), 14.88 (s), 13.15 (s). LCMS:  $m/z$  [M+H] $^+$ , calcd: 525.22, found: 525.2173. ESI-HRMS:  $m/z$  [M+Na] $^+$ , calcd: 547.2064, found: 547.2077.

### 3.4 Structures of biotin-rhodamine azide and the negative probe

The click reporter biotin-rhodamine azide (Biotin-TER-N<sub>3</sub>) and the control negative probe (NP) were synthesized as reported<sup>1, 23</sup>. The purpose of NP in experiments is to reduce false-positive hits, which are intrinsic and unavoidable<sup>24</sup>.



*3-(3-(but-3-yn-1-yl)-3H-diazirin-3-yl)-N-phenylpropanamide*

Figure 3: Structures of biotin-rhodamine azide and the negative probe

### 3.5 Cell culture and western blot

Cell lines were provided by the National Cancer Institute Developmental Therapeutics Program (NCI-60). HepG2, HeLa, MCF-7, NIH3T3, HT29 cells were cultured in Dulbecco's modified Eagle medium (DMEM; Invitrogen, Carlsbad, CA) containing 10% heat-inactivated fetal bovine serum (FBS; Invitrogen), 100 units/mL penicillin and 100 µg/mL streptomycin (Thermo Scientific), and maintained in a humidified 37 °C incubator with 5% CO<sub>2</sub>. For WB experiments, samples from respective cells were resolved by sodium doceyl sulphate – polyacrylamide gel electrophoresis (SDS-PAGE) and transferred to poly(vinylidene difluoride) membranes. Membranes were then blocked with 3% bovine serum albumin (BSA) in TBST (0.1% Tween in Tris-buffered saline) for 1 h at room temperature. Subsequently, membranes were incubated with the corresponding primary antibody for another hour, after which they were washed with TBST (4×10 min) and then incubated with an appropriate secondary antibody for 1 hour. Finally, after blots were washed again with TBST thrice, they were developed with SuperSignal West Dura Kit (Thermo Scientific).

### *3.6 TNKS1/2 and bacterial lysate labelling with probe XA1*

As reported<sup>25</sup>, catalytic domains of TNKS1/2 fused with His-tags were acquired through protein over-expression in *E.Coli* transformed with a plasmid carrying the target gene, and then purified by nickel affinity beads. To 1 µg TNKS1/2 was added equal volume of either XA1 in different concentrations with or without excess competitors, or the control negative probe, followed by incubation for 1 hour at r.t.. Subsequently upon UV irradiation (~ 350 nm) for 20 min, the solutions were added in click chemistry master reagents. Reaction was stopped 2 hours later by adding 6×SDS loading dye and heated to 95 °C for 10 min. The resulting proteins were resolved by SDS-PAGE. In-gel fluorescence scanning (FL) was used to visualize the labeled protein bands. Both in-gel fluorescence scanning and coomassie brilliant blue staining (CBB) were always carried out on the gels upon SDS-PAGE separation of labeled samples

To acquire bacterial lysate, pellets of TNKS1/2 over-expression induced *E.Coli* were re-suspended in N-(2-hydroxyethyl)piperazine-N-2-ethanesulfonic acid (HEPES) buffer (25 mM HEPES, 150 mM NaCl, 2 mM MgCl<sub>2</sub>, pH 7.5) containing 50 µM PMSF, and sonicated (10 min of 5 s on and 5 s off, at 30% amplitude) to completeness. Undissolvable debris was removed through centrifugation at 13000 rpm, 4 °C for 10 min. The supernatant, of which the total protein concentration was quantified by Bio-

Rad assay (Bio-Rad USA), was stored at -20 °C for subsequent labelling experiments. Lysate labelling experiments were performed in a similar way as above except that instead of 1 µg TNKS1/2, 20 µg bacterial lysates were employed.

### *3.7 Cytotoxicity assay of the probe CA1 and wild-type camptothecin*

As reported, camptothecin displays nanomolar potency in cytotoxicity against many human cell lines, with IC<sub>50</sub> values ranging from 37 nM to 48 nM<sup>15</sup>. In order to demonstrate that incorporation of minimalist onto camptothecin has little effect on its bioactivity, cytotoxicity assay experiments were conducted. The procedure was based on the published protocol<sup>15</sup>, however, by the aid of XTT colorimetric assay kit (Roche). In brief, cells were grown to 70-80% confluence in 96-well plates under the conditions described above. The medium was aspirated, and then washed with PBS, and treated in triplicate, with 0.1 mL of the medium containing different concentrations of probes (1-20 µM, diluted from DMSO stocks whereby DMSO never exceeded 1% in the final solution) or drug (1-20 µM, as a positive control). The same volume of DMSO was used as a negative control. Reference wells were treated with 10 nM STS. Fresh medium, along with the probes and corresponding drug, were added every 24 h. After a total treatment time of 48 h, cell viability were assayed using the XTT colorimetric kit (Roche) following manufacturer's guidelines (read at 450 nm). Data represent the average (s.d. for three trials).

### *3.8 In vitro and in situ proteome labelling in HepG2 cell lines*

To acquire protein lysates, cells were washed thrice with cold PBS, harvested through detachment either by 1× trypsin or by a cell scraper, and centrifugation. Cell pellets were washed with PBS thrice and lysed with HEPES buffer containing 0.1% NP-40 and 50 µM PMSF. The lysate, of which the total protein concentration was quantified by Bio-Rad assay (Bio-Rad USA), was stored at -20 °C for subsequent labelling experiments.

The procedure was in accordance with the previously reported<sup>1</sup>, however with minor adjustments. For *in vitro* labelling, to 50 µg of cell lysate was added in either the probes with or without excess amount of competitor, or the control NP, or the blank control DMSO. The resulting solutions were UV-irradiated (350 nm) for 20 mins and subsequently added in click master reagent. After 2 hrs incubation at r.t., the solutions

were added in pre-chilled acetone (10 times in volume; incubation for 1hr at -20°C). Precipitated protein was recovered by centrifugation (13000 rpm, -4 °C, 10 mins), washed by pre-chilled methanol thrice and re-dissolved by loading dye with gentle heating at 95 °C for 10mins. ca. 20 µg per gel lane of proteins were separated by SDS-PAGE (10% gel) and then visualized by in-gel fluorescence scanning. For *in situ* labelling, cells were grown to 80–90% confluence in 12-well plates under conditions described above. The medium was discarded, and cells were washed thrice by cold PBS. Each well was treated with 0.5 mL of the DMEM-containing either probes in the presence or absence of excess competitor (diluted from DMSO stocks whereby DMSO never exceeded 1% in the final solution) or the control NP, or DMSO. After 3 h of incubation at 37 °C/5% CO<sub>2</sub>, the medium was aspirated, and cells were washed gently with PBS (2×) to remove excessive probes, followed by UV irradiation for 20 min on ice. Eventually, the cell pellets were re-suspended in PBS (50 µL), homogenized by sonication, and diluted to 1 mg/mL with PBS. All subsequent procedures were similar to those of *in vitro* experiments.

### 3.9 Target protein pull-down and western blotting

In order to identify the potential cellular targets for the probes and their parental bioactive molecules, pull-down and western blotting experiments were conducted. Various mammalian cell lines, including but not limited to HepG2, HeLa, MCF-7, NIH3T3, HT29 cell lines were utilized when necessary. The general pull-down procedure was found in the formerly published<sup>1</sup> and further optimized as follows: Fresh whole cell lysates were prepared and their protein concentration determined, as described earlier. For *in vitro* pull-down experiments, cellular lysates (2 mg) were filled with 200 µL 5× HEPES buffer (125 mM HEPES, 750 mM NaCl, 10 mM MgCl<sub>2</sub>, pH 7.5), and the reaction volume was adjusted to 1 mL with milli-Q water. Subsequently, a solution of probe (1 µM, 5 µL of a 200 µM stock solution or 5 µM, 5 µL of a 1 mM stock solution) was added, and equilibrium was reached for 2 hrs at room temperature. Afterwards, the reaction mixture was UV-irradiated (350 nm) for 30 mins, followed by treatment with the click master reagents for 3 hrs. After acetone precipitation as described earlier, protein pellets were resolubilized in 1% SDS in PBS with brief sonication. This re-suspended sample was then incubated with avidin-agarose beads (100 µL/mg protein) 3 hrs at room temperature or overnight at 4 °C. After centrifugation,

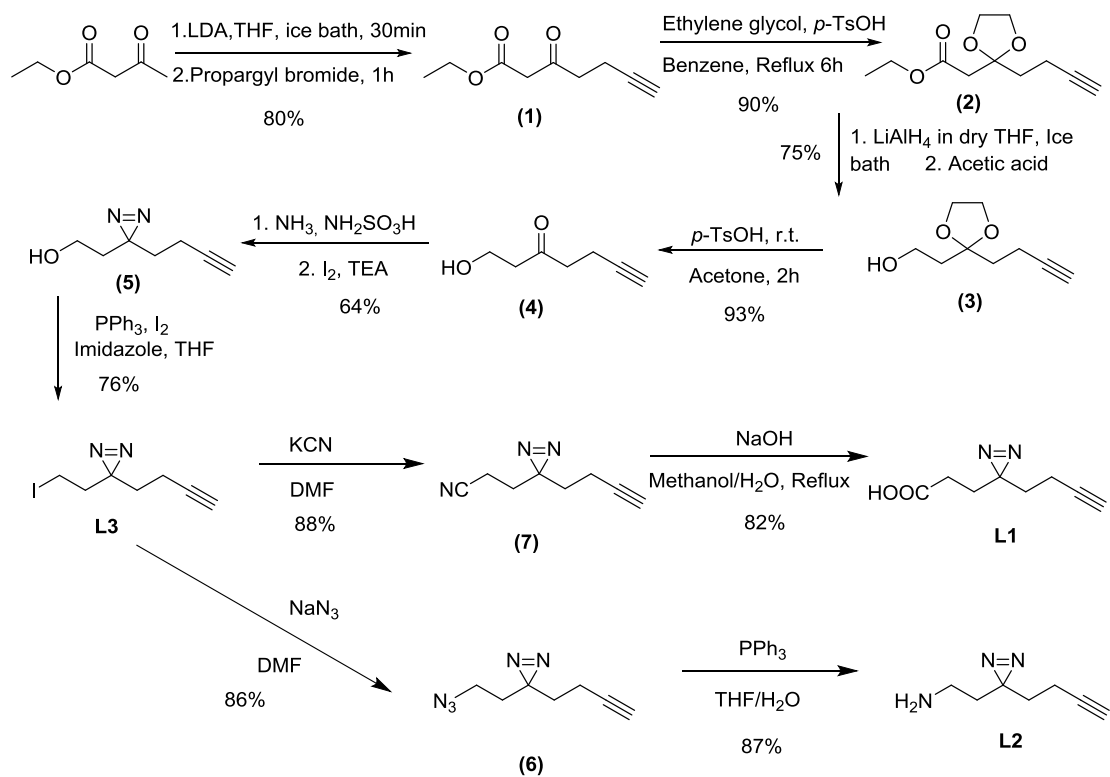
supernatant was discarded and the beads were firstly washed with 0.1% SDS once, then cold PBS for 4 times, and finally boiled in 1× SDS loading buffer (200 mM Tris, 400 mM DTT, 8% SDS, pH 6.8) for 15 min. Control PD using the NP (5 µM, 5 µL of a 1 mM stock solution) were carried out concurrently. For *in situ* PD, 1 mL DMEM contacting the probes (1 µM, 5 µL of a 200 µM stock solution or 5 µM, 5 µL of a 1 mM stock solution) was directly added to live cells grown in 6-well dishes, followed by incubation at 37 °C/5% CO<sub>2</sub> for 5 h, removal of the medium, and washing thrice gently with PBS. Cells were then UV irradiation (~350 nm) for 30 min on ice. Upon harvest by cell scraper, the cell pellets were re-suspended in PBS (50 µL), homogenized by sonication, and diluted to 1 mg/mL with PBS. The labeled lysates were then subjected to click reaction with biotin-rhodamine azide, and all subsequent experiments were carried out as above described. Control PD using the NP (5 µM, 5 µL of a 1 mM stock solution) was also carried out concurrently. WB experiments were carried out as previously described using the corresponding antibodies.

### 3.10 Cellular imaging

Cellular imaging experiments were performed so as to demonstrate the potential utility of cell-permeable probes to image their cellular targets. The overall procedure was similar to the previously reported<sup>1</sup>. To put it concisely, HepG2 cells were seeded in glass bottom dishes (Mattek) and cultured to 70%-80% confluency. Medium was discarded and cells were gently washed thrice with PBS. Subsequently, cells were treated with 0.5 mL DMEM containing either probes in different concentrations in the presence or absence of competitors, or the control NP. Upon incubation for 2 hrs, medium was removed and cells were washed thrice with PBS, followed by UV-irradiation for 25 mins. Cells were then fixed for 30 mins at room temperature with 3.7% formaldehyde in PBS, washed with PBS thrice and permeabilized with 0.1% Triton X-100 in PBS for 10 mins. Afterwards, cells were blocked by 2% BSA in PBS for 30 mins, washed by PBS thrice and treated with click master reagents for 3 hr at room temperature under vigorous shaking. For co-localization experiments, firstly cells were further incubated with target-specific antibodies for 1 h at room temperature (or overnight at 4 °C), followed by washing thrice with PBS. Next, cells were incubated with fluorescein isothiocyanate (FITC)-conjugated anti-rabbit/mouse IgG for 1 h, following by washing again. Finally, imaging and images processing were conducted as described earlier.

## 4. Results and discussion

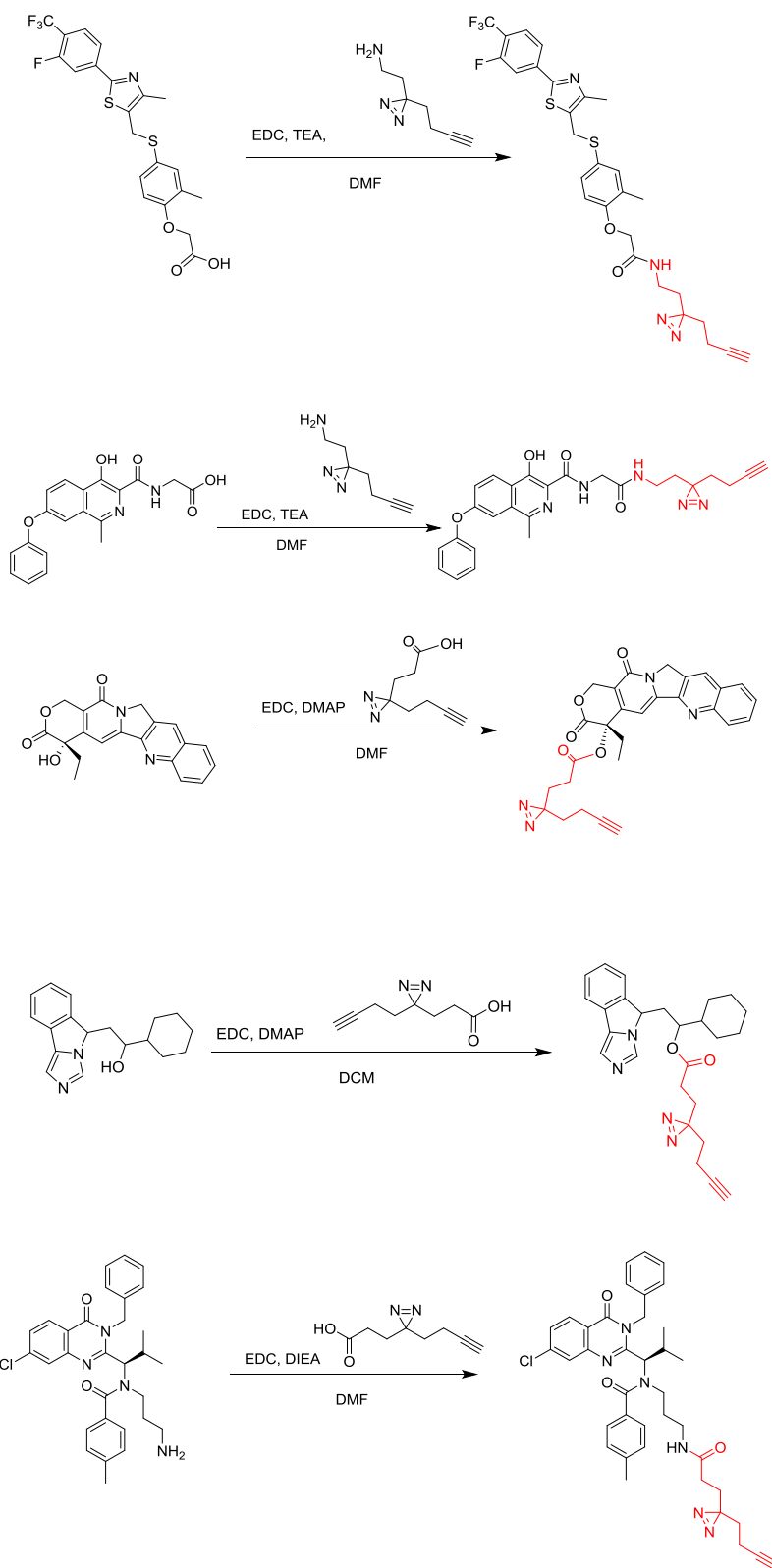
### 4.1 Linker synthesis scheme

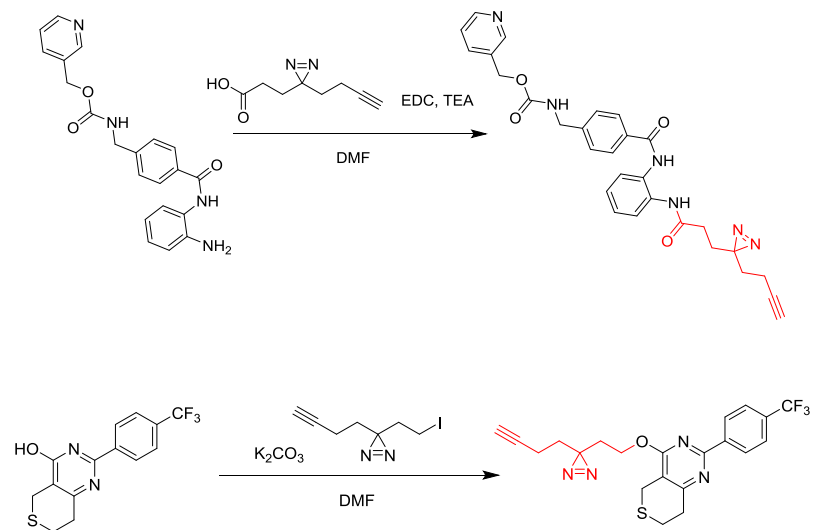


Scheme 1: Synthetic route of minimalist linker L1-L3.

Following published protocol<sup>1, 26</sup>, synthesis of the “minimalist” linkers started with commercially available ethyl acetoacetate. By applying two equivalents of LDA to deprotonate the terminal methyl, followed by nucleophilic substitution, the terminal alkyne handle was readily installed. Next, through acetal protection and LAH reduction, the ester group was converted to an alcohol. After deprotection, the carbonyl was transformed into a diazirine group by two consecutive reactions: carbonyl substitution and oxidation of diazo ring. Subsequently, the hydroxyl group was substituted to a better leaving group, an iodine atom was easily substituted by other nucleophiles-cyanide and azide. Upon hydration, construction of L1 and L2 completed. The yield for each step was shown in the scheme.

#### 4.2 Probe synthesis scheme





Scheme 2: Coupling scheme between the bioactive molecules and the “minimalist” linkers.

With all three “minimalist” linkers in hand, they were installed into several bioactive molecules so as to construct the probes XA1, GW1, FG1, CA1, NL1, IS1 and EN1. Coupling between acids and amines was facilitated by carboxyl activating reagent EDC. EDC converts the acid to an unstable o-acylisourea intermediate, which upon nucleophilic addition of amine, would readily collapse to form the product-amide. The following figure illustrates the role of EDC.

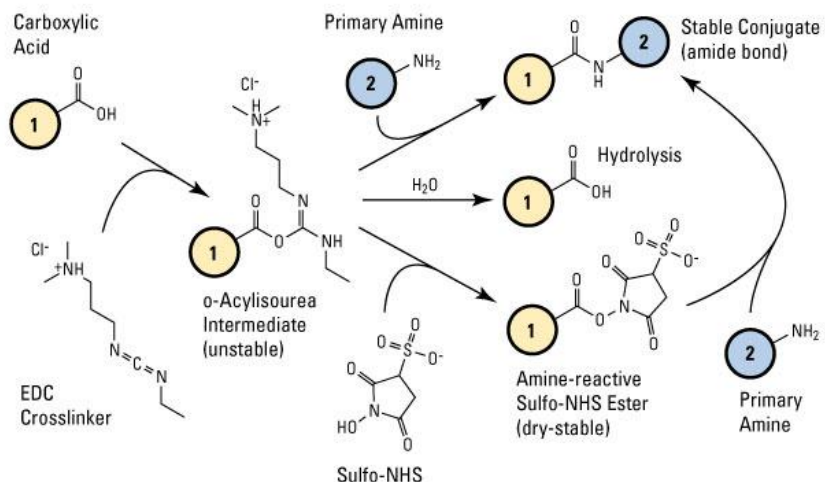
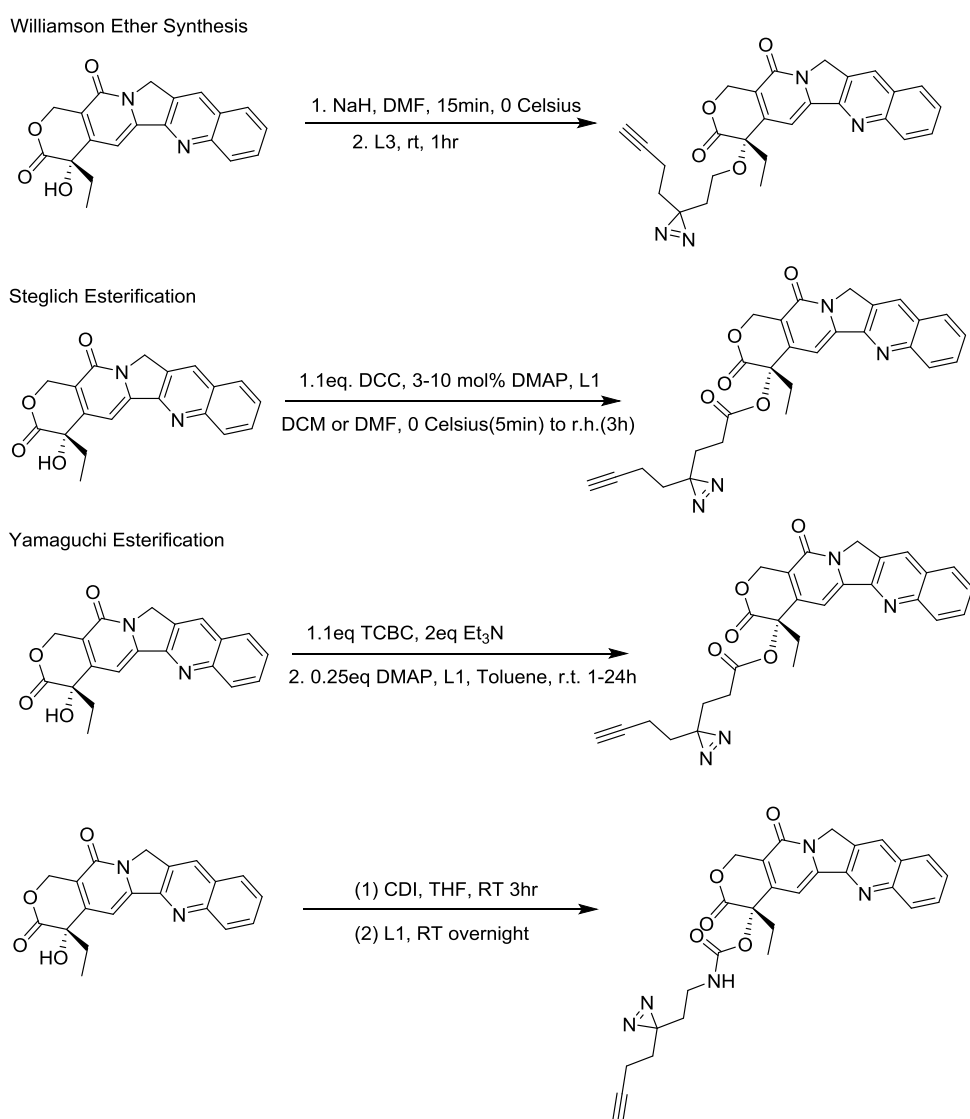


Figure 4: Mechanism of carboxyl activation by EDC<sup>a</sup>

<sup>a</sup> Illustration retrieved 01/04/2014 from <http://www.piercenet.com/method/carbodiimide-crosslinker-chemistry>

Coupling between acids and alcohol were a bit more difficult since acyl group was no better a leaving group in O-acylisourea. Normal acid or base catalysed ester formation (e.g. Fischer esterification) was hardly applicable since the linkers were sensitive to heat. Mitsunobu reaction was ruled out since it would invert a chiral centre in the case of camptothecin. Originally, four reactions were proposed for the coupling between camptothecin and the minimalist linkers: Steglich esterification, Yamaguchi esterification, CDI coupling and an alternative way to form an ester by Williamson ether synthesis (see Scheme 3). It turned out Steglich esterification performed well, though EDC was employed instead of DCC in our case. DMAP serves as a base catalyst and an acyl transfer reagent to convert the O-acylisourea to pyrimidine bonded amide, which consists of an excellent leaving group.



Scheme 3: Proposed coupling scheme between camptothecin and “minimalist” linkers

Installation of a “minimalist” linker on XAV939 involves a simple substitution reaction under mild basic condition. As we can see, all the coupling reactions performed were robust, simple and high yielding. This promising feature makes our “minimalist” linker widely applicable in any other bioactive molecules. All probes were fully characterized by LCMS, ESI-HRMS, <sup>1</sup>H NMR, <sup>13</sup>C NMR (see supporting information) before downstream biological experiments.

#### *4.3 TNKS1/2 overexpression and purification*

Luckily, our lab hoards plasmids carrying TNKS1/2 gene (catalytic domains only). The plasmids were transformed into *E.Coli*. Upon induction and overexpression, TNKS1/2 proteins were subsequently purified. The size of TNKS1 was ca. 28kDa while that of TNKS2 was ca. 26kDa<sup>22</sup>. Apparently, TNKS2 was much purer than TNKS1. TNKS2 was employed in pure protein and bacterial lysate labelling experiments.

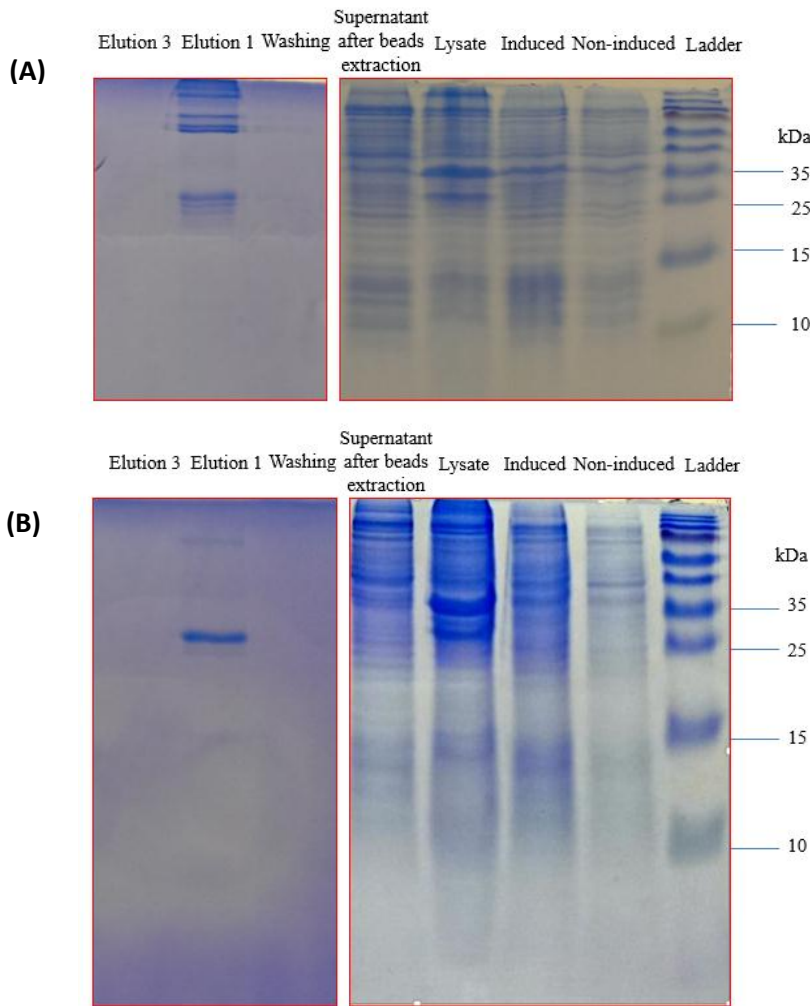


Figure 5: TNKS1 (A) and TNKS2 (B) purification. Lanes from right to left shows SDS-PAGE resolution of protein ladder, non-induced *E.Coli* pellet, induced *E.Coli* pellet, induced *E.Coli* lysate, supernatant after extraction by nickel affinity beads, wash waste, first elution and last elution by elution buffer containing high concentration of imidazole.

#### 4.4 Enzymatic activity assay of XA1

With seven probes in hand, the first task was to evaluate whether modifications on the parental bioactive molecules would severely affect their biological activities. Several experiments would evaluate this issue including enzymatic activity assay, XTT-based cytotoxicity assay if suitable. Taken availability and feasibility into consideration, TNKS2 enzymatic activity assay for XA1 and XTT-based cytotoxicity assay for CA1 were proposed. By replacing the PARP1 protein stock with freshly prepared TNKS2 (a.k.a PARP5b, which has similar enzymatic function with other

PARP family) proteins in previously purchased PARP1 assay kit, IC<sub>50</sub> measurement was carried out for XA1. XA1 was determined to have an IC<sub>50</sub> value of 52.82nM. The IC<sub>50</sub> of wide-type XAV-939 was reported to be 4nM<sup>15</sup>. The change was large but still within acceptable range. More importantly, the design had some drawbacks. For a credible comparison, XAV-939 and XA1 should have been measured under the same experimental conditions and statistically a large set of data points would be more convincing. However, due to lack of assay kits, these were not re-performed. Hopefully, upon purchase of new assay kit, this will be conducted in a scientifically appropriate way.

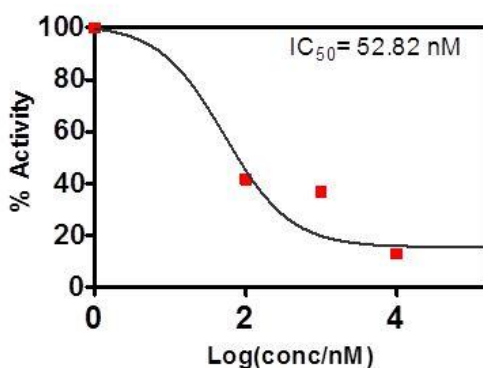


Figure 6: IC<sub>50</sub> measurement of XA1

#### 4.5 In vitro TNKS2 and bacterial lysate labelling

Next, we assessed whether XA1 served as an effective AfBP for covalent labelling of TNKS1/2 *in vitro*. Dose-dependent experiments were carried out by varying the concentration of XA1 in the labelling reaction. In gel fluorescence scanning results (see figure 7) clearly show that as the concentration of XA1 increases, the fluorescence increases as well. Meanwhile the control NP doesn't show detectable fluorescence for the concerned band. Therefore, XA1 does show high specificity towards TNKS1/2.

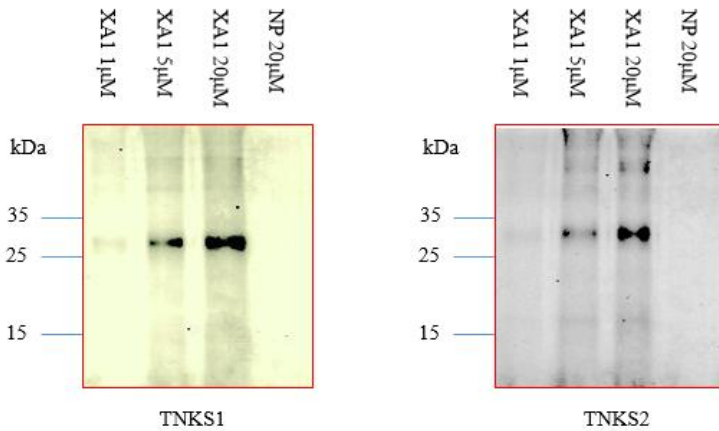


Figure 7: TNKS1/2 labelling. Lanes from left to right shows TNKS1/2 labelled by 1 $\mu$ M XA1, 5 $\mu$ M XA1, 20 $\mu$ M XA1 and 20 $\mu$ M NP

XA1's specificity was re-verified by TNKS1 labelling in bacterial lysate. In this experiment, besides the NP, all other six probes served as negative controls as well since ideally they possess no activities towards TNKS1 and will not label TNKS1 in cellular matrix. In parallel, competition labelling of XA1 were carried out under 10-times excess amount of its WT-XAV939. Such an excess amount would nearly compete off all XA1 let alone that XA1 may have a reduced affinity towards TNKS1 compared to XAV939. Meanwhile, competition would reveal whether XA1 truly binds to the active site of TNKS1 since if it anyhow encounters TNKS1 and labels it, competition of WT will not affect its labelling. Apparently, in gel fluorescence scanning results (see figure 8) indicate that XA1 labels TNKS1 in a dose dependent manner, specific and affinitive towards the active pocket of TNKS1. Incorporation of the “minimalist” linker into XAV-939 results in negligible derivation from its biological activity, however confers superb potential as an AfBP.

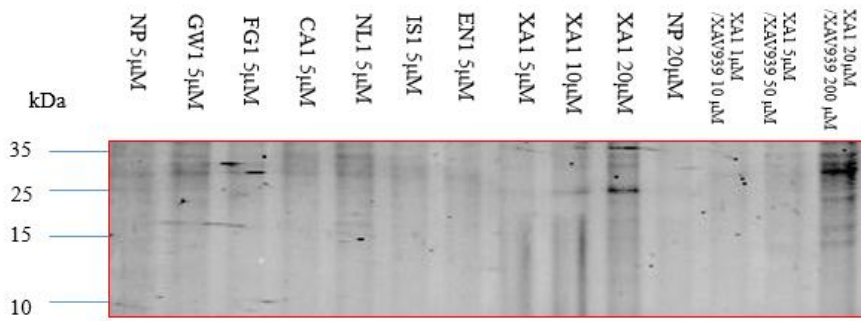


Figure 8: Bacterial lysate labelling. Lanes from left to right show bacterial lysate labelling by NP 5 $\mu$ M, GW1 5 $\mu$ M, FG1 5 $\mu$ M, CA1 5 $\mu$ M, NL1 5 $\mu$ M, IS1 5 $\mu$ M, EN1 5 $\mu$ M, XA1 1 $\mu$ M, XA1 5 $\mu$ M, XA1 20 $\mu$ M, NP 20 $\mu$ M, XA1 1 $\mu$ M with XAV939 10 $\mu$ M, XA1 5 $\mu$ M with XAV939 50 $\mu$ M and XA1 20 $\mu$ M with XAV939 200 $\mu$ M

#### 4.6 *In vitro* and *in situ* HepG2 proteome labelling

Next, *in vitro* and *in situ* HepG2 proteome labelling were carried out. In gel fluorescence scanning results may suggest that probes are not specific since many labelled bands appeared for each probe. However, given that the molar amount of probes is far more enough than that of their target proteins and the lifetime of carbene intermediate is relatively long, it is likely for probes to label other proteins as well, especially those abundant proteins. If we observe carefully, there are subtle differences in the intensity and band locations. At least, there are three clues we can draw from these experiments. Firstly, the probes do label proteins and the click chemistry works well. Secondly, under WT-competitive conditions, certain bands do show reduced intensity, which indicates probes do have certain affinity towards some active proteins. Lastly, *in situ* experiments validate the probes' permeability.

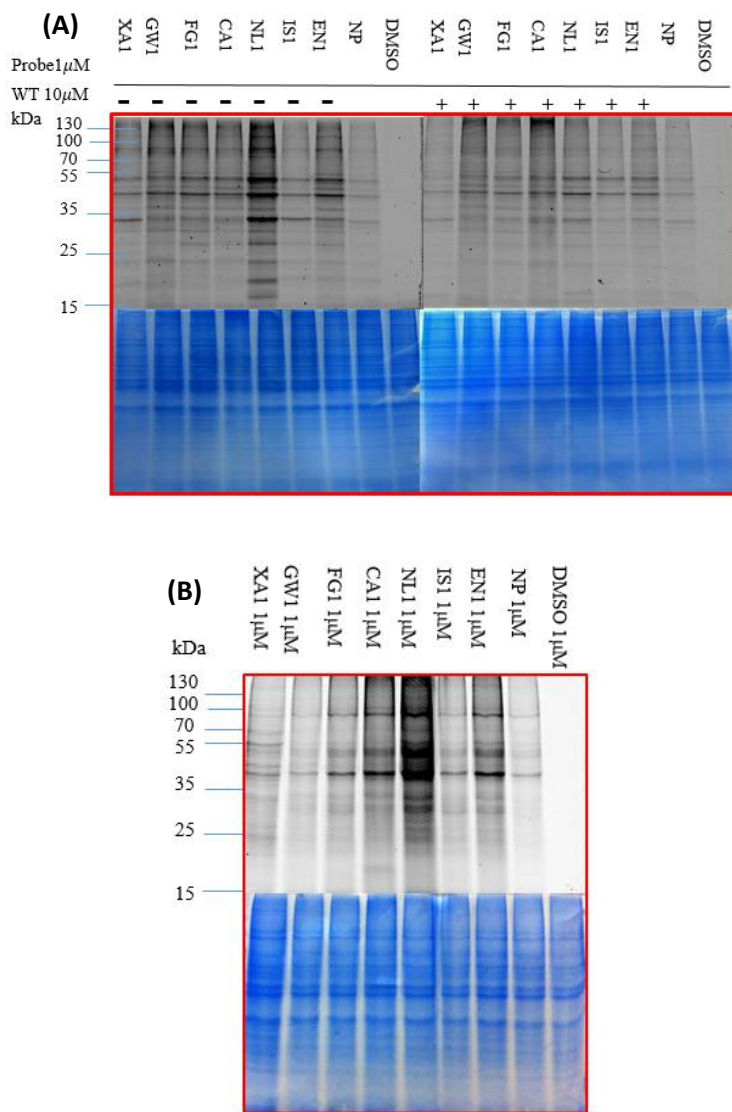


Figure 9: *In vitro* (A) and *in situ* (B) proteome reactivity profiles in HepG2 cell lines with 7 probes in the presence or absence of competitors (only for *in vitro*), NP and DMSO.

#### 4.7 Pull down and western blot

In order to further verify the cell-permeable and clickable nature of the probes and their ability to tag the respectively known targets, endogenous proteome labelling in both cell lysate and live cells were conducted, followed by large-scale pull-down and validation through western blotting experiments. To date, four of the probes have successfully pulled down their target proteins *in vitro*. Though *in situ* experiments are required for thorough proof, the same results are highly expected since there is no issue for probe's cell permeability as shown in *in situ* HepG2 proteome profiling. These results strongly suggest that the “minimalist” tagging strategy is widely applicable

across various classes of proteins. Due to limited time, unfinished experiments will be included in future works.

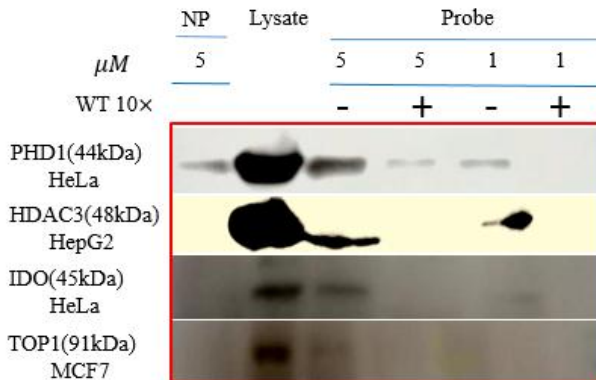


Figure 10: *in vitro* PD/WB for 4 of the probes FG1, EN1, NL1 and CA1

## 5. Conclusion

We have successfully constructed several A<sub>f</sub>BPs by the method of “minimalist” tagging. The coupling between the bioactive molecules and the “minimalist” linkers is invariantly robust, simple and high yielding, making the “minimalist” approach widely applicable for any bioactive molecules. More importantly, these probes are cell-permeable, clickable and do not significantly alter the biological activities of their parental bioactive molecules. Their application in ABPP was demonstrated by sophisticated biological experiments. Firstly, from enzymatic activity assay and XTT-based cytotoxic assay, we confirmed that our probes have similar cell-permeability and biological effects as the WT bioactive molecules. Next, through protein labelling and bacterial lysate labelling experiments with or without competitors, we proved that the probes are specific and affinitive towards the active sites of their target proteins. *In vitro* and *in situ* HepG2 proteome profiling clearly indicate that the two-step labelling and the click chemistry worked extraordinarily well. Upon successful PD/WB, we further verified the cell-permeable and clickable nature of the probes and their ability to tag the respectively known targets and some potential off-targets that are to be vigorously validated by LCMS/MS in further studies. In conclusion, our extensive studies strongly suggest that the “minimalist” small molecule tagging approach readily spans various protein classes and greatly expands the proteome coverage of ABPP.

## 6. Future work

In order to end the whole story of this project, the following experiments are to be performed at least for this project: *in situ* PD/WB, cellular imaging, XTT based cytotoxicity assay, TNKS1/2 enzymatic activity assay.

Despite all the excellent characteristics of our “minimalist” linkers, there are still a few problems not addressed. Firstly, though the three functionalised version could potentially cover almost all coupling reactions, some bioactive molecules without carboxyl, alcohol, amine group or those of which the incorporable site is critical revealed by structure-activity relationship are not suited for the minimalist tagging strategy. One probable solution would be to retrieve and utilise more versatile coupling reactions from synthetic chemistry, such as alky/aryl H activation reactions<sup>27</sup>. Secondly, intrinsic retard of diazirine activation by long-wave UV poses non-specific labelling issue. This problem was partially tackled before when Brunner and co-workers reported the design of 3-aryl-3-(trifluoromethyl)-3H-diazirine<sup>28</sup>. Due to the extremely high electron-withdrawing effect of trifluoromethyl group, slowness and side reactions were erased. However, the bulkiness of the aryl group prevented its further employment in designing A/BPs. Lastly, copper, which is used as a catalyst in ligation reaction, is proved to have cell toxicity<sup>29</sup>, this may hamper the development of this strategy for real time live cell imaging. By overcoming all these challenging problems, hopefully a new general approach for ABPP would surface.

## 7. Acknowledgements

I would like to express my special appreciation and thanks to my supervisor, Professor Dr. Yao Shao Qin, without your unwavering support and valuable advice, I would not be able to accomplish my FYP project. I would also like to thank my mentor, Dr. Li Zhengqiu, you have been an excellent accompany especially when I was enduring hardship in experiments. I feel grateful for all your brilliant suggestions and comments. Peng Bo and Chelsea, I would like to thank you as well, for guiding me through the biological experiments. Words cannot express how grateful I am to all those who have in one way or another helped me, including but not limited to lab members, technicians, staffs in the department and the university. Last but not least a special thanks goes to my family and friends, especially Dion and Sandra for their encouragement throughout the whole course of this project.

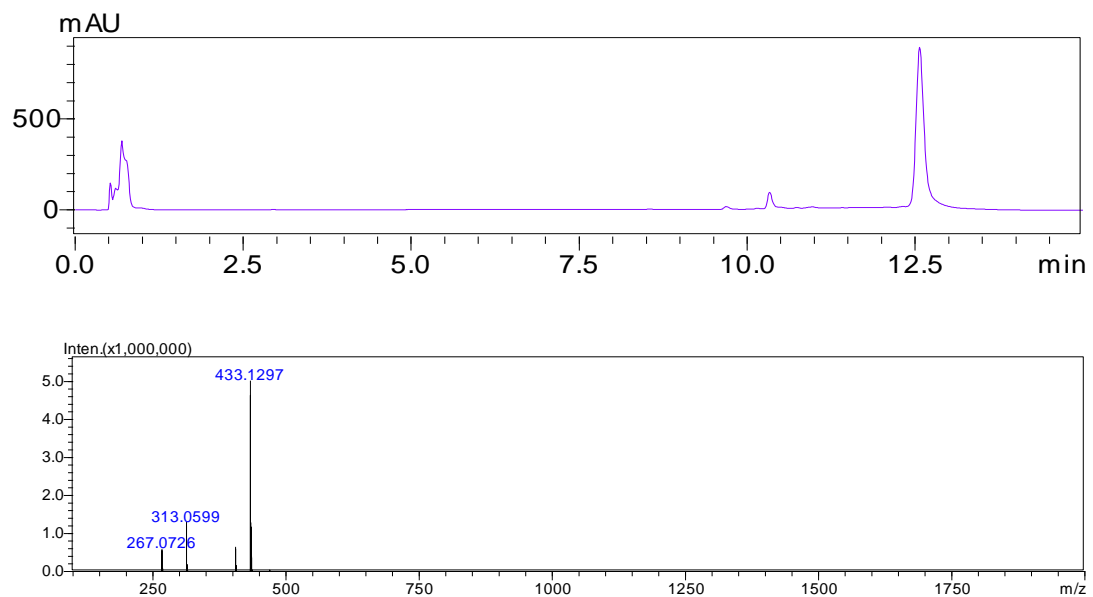
## 8. References

1. Z. Li, P. Hao, L. Li, C. Y. Tan, X. Cheng, G. Y. Chen, S. K. Sze, H. M. Shen and S. Q. Yao, *Angew. Chem. Int. Ed.*, 2013, **52**, 8551-8556.
2. M. J. Evans and B. F. Cravatt, *Chem. Rev.*, 2006, **106**, 3279-3301.
3. B. F. Cravatt, A. T. Wright and J. W. Kozarich, *Annu. Rev. Biochem.*, 2008, **77**, 383-414.
4. K. A. Kalesh, H. Shi, J. Ge and S. Q. Yao, *Org. Biomol. Chem.*, 2010, **8**, 1749-1762.
5. Y. Su, J. Ge, B. Zhu, Y.-G. Zheng, Q. Zhu and S. Q. Yao, *Curr. Opin. Chem. Biol.*, 2013, **17**, 768-775.
6. E. Vodovozova, *Biochemistry (Moscow)*, 2007, **72**, 1-20.
7. Y. Tanaka, M. R. Bond and J. J. Kohler, *Molecular BioSystems*, 2008, **4**, 473-480.
8. P. P. Geurink, L. M. Prely, G. A. van der Marel, R. Bischoff and H. S. Overkleeft, in *Activity-Based Protein Profiling*, Springer, 2012, pp. 85-113.
9. H. Shi, C. J. Zhang, G. Y. Chen and S. Q. Yao, *J. Am. Chem. Soc.*, 2012, **134**, 3001-3014.
10. J. Rayo, N. Amara, P. Krief and M. M. Meijler, *J. Am. Chem. Soc.*, 2011, **133**, 7469-7475.
11. A. L. Garner, J. Yu, A. K. Struss, C. A. Lowery, J. Zhu, S. K. Kim, J. Park, A. V. Mayorov, G. F. Kaufmann and V. V. Kravchenko, *Bioorg. Med. Chem. Lett.*, 2011, **21**, 2702-2705.
12. Q. Wang, T. R. Chan, R. Hilgraf, V. V. Fokin, K. B. Sharpless and M. Finn, *J. Am. Chem. Soc.*, 2003, **125**, 3192-3193.
13. E. Saxon, J. I. Armstrong and C. R. Bertozzi, *Org. Lett.*, 2000, **2**, 2141-2143.
14. V. V. Rostovtsev, L. G. Green, V. V. Fokin and K. B. Sharpless, *Angew. Chem.*, 2002, **114**, 2708-2711.
15. M. J. Luzzio, J. M. Besterman, D. L. Emerson, M. G. Evans, K. Lackey, P. L. Leitner, G. McIntyre, B. Morton, P. L. Myers and M. Peel, *J. Med. Chem.*, 1995, **38**, 395-401.
16. R. C. Dregalla, J. Zhou, R. R. Idate, C. L. Battaglia, H. L. Liber and S. M. Bailey, *Aging (Albany NY)*, 2010, **2**, 691.
17. K. Bruegge, W. Jelkmann and E. Metzen, *Curr. Med. Chem.*, 2007, **14**, 1853-1862.
18. R. M. Mario, F. A. Jaipuri, J. Waldo, S. Kumar, J. Adams, C. V. Allen, A. M. Flick, D. Munn, N. Vahanian and C. J. Link, *Cancer Res.*, 2013, **73**.
19. T. Tatamiya, A. Saito, T. Sugawara and O. Nakanishi, *AACR Meeting Abstracts*, 2004, **2004**, 567.
20. L. Lad, L. Luo, J. D. Carson, K. W. Wood, J. J. Hartman, R. A. Copeland and R. Sakowicz, *J. Biochem.*, 2008, **47**, 3576-3585.
21. M. L. Sznajzman, C. D. Haffner, P. R. Maloney, A. Fivush, E. Chao, D. Goreham, M. L. Sierra, C. LeGrumelec, H. E. Xu, V. G. Montana, M. H. Lambert, T. M. Willson, W. R. Oliver, Jr. and D. D. Sternbach, *Bioorg. Med. Chem. Lett.*, 2003, **13**, 1517-1521.
22. E. Wahlberg, T. Karlberg, E. Kouznetsova, N. Markova, A. Macchiarulo, A. G. Thorsell, E. Pol, Å. Frostell, T. Ekblad and D. Öncü, *Nat. Biotech.*, 2012, **30**, 283-288.
23. X. Cheng, L. Li, M. Uttamchandani and S. Q. Yao, *Chem. Commun.*, 2014, **50**, 2851-2853.
24. K. Sakurai, M. Tawa, A. Okada, R. Yamada, N. Sato, M. Inahara and M. Inoue, *Chem.-Asian. J.*, 2012, **7**, 1567-1571.
25. L. Lehtiö, R. Collins, S. van den Berg, A. Johansson, L. G. Dahlgren, M. Hammarström, T. Helleday, L. Holmberg-Schiavone, T. Karlberg and J. Weigelt, *J. Mol. Bio.*, 2008, **379**, 136-145.
26. K. Hayakawa, M. Yodo, S. Ohsuki and K. Kanematsu, *J. Am. Chem. Soc.*, 1984, **106**, 6735-6740.
27. X. Chen, K. M. Engle, D. H. Wang and J. Q. Yu, *Angew. Chem. Int. Ed.*, 2009, **48**, 5094-5115.
28. J. Brunner and G. Semenza, *J. Biochem.*, 1981, **20**, 7174-7182.
29. N. Aston, N. Watt, I. Morton, M. Tanner and G. Evans, *Human & experimental toxicology*, 2000, **19**, 367-376.

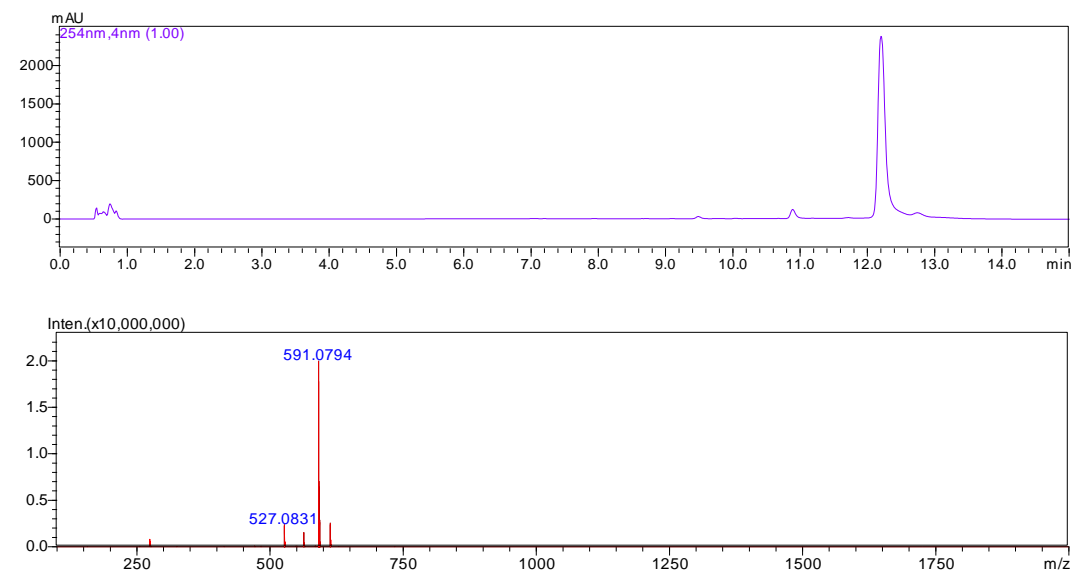
## 9. Supporting Information

*LCMS and ESI-HRMS data*

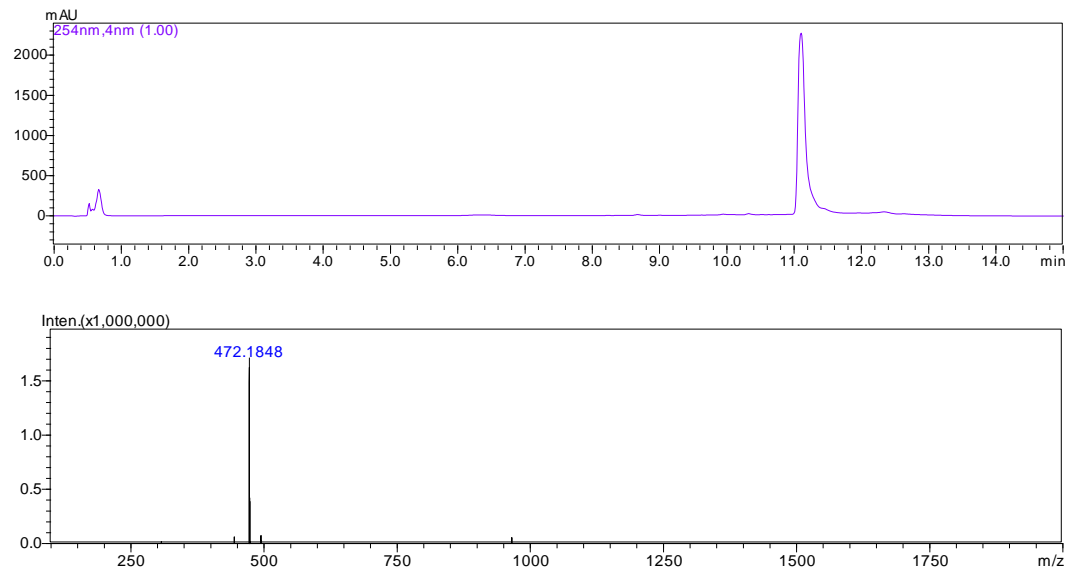
XA1



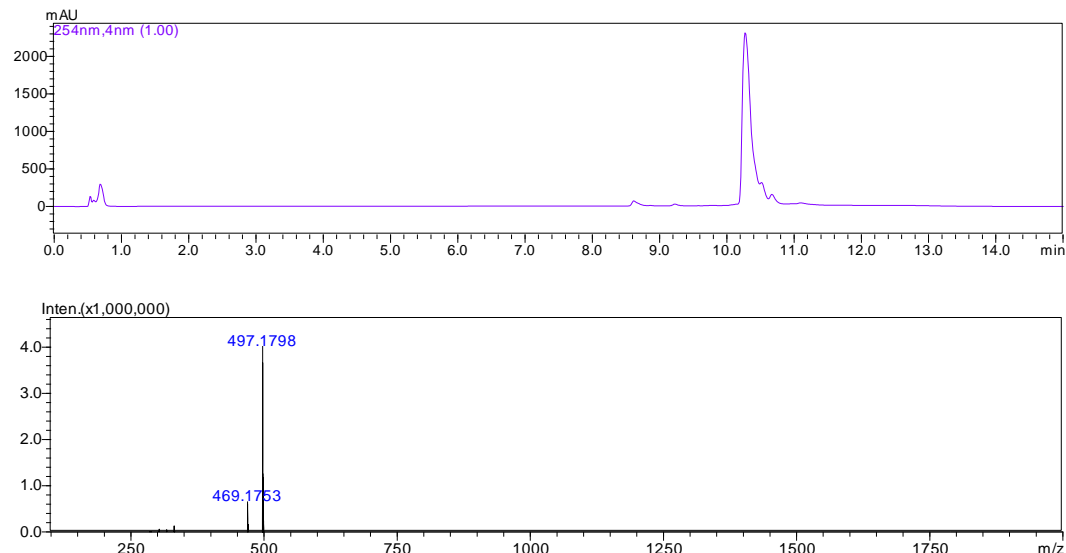
GW1



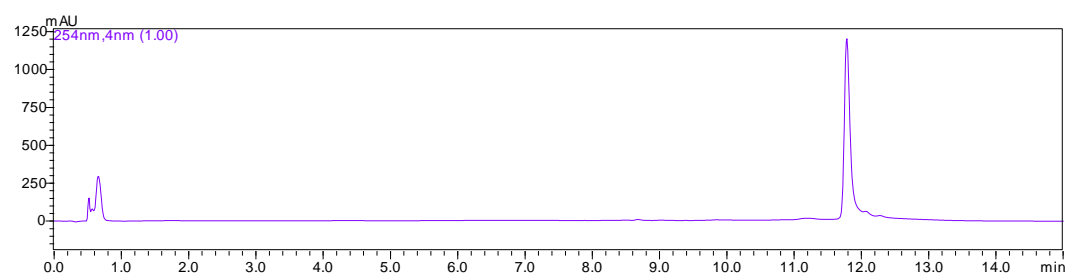
FG1



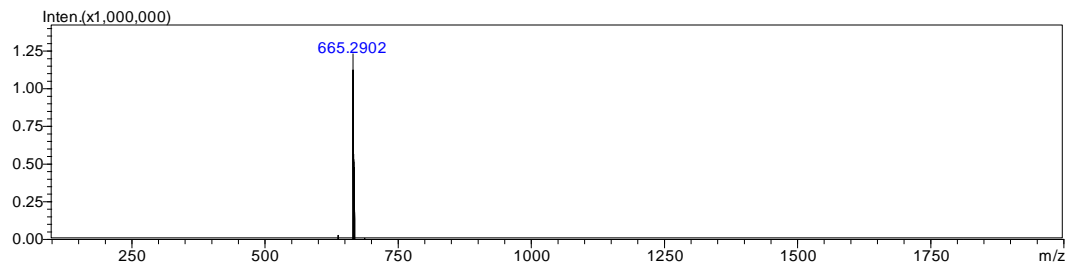
CA1



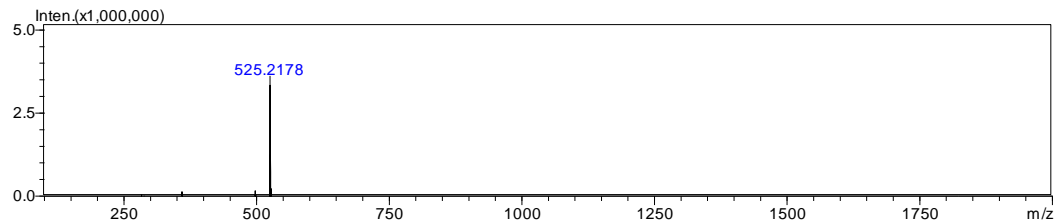
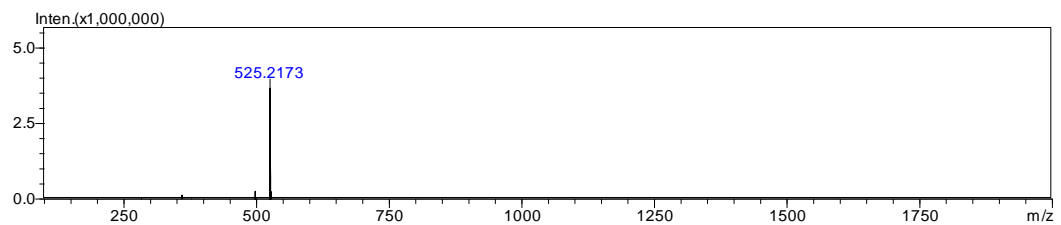
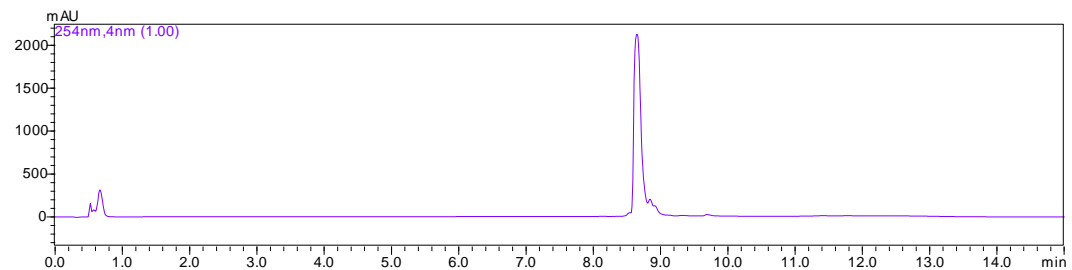
IS1



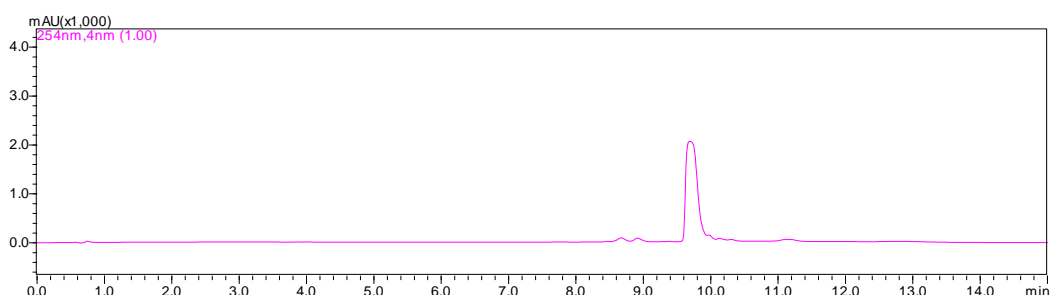
S2



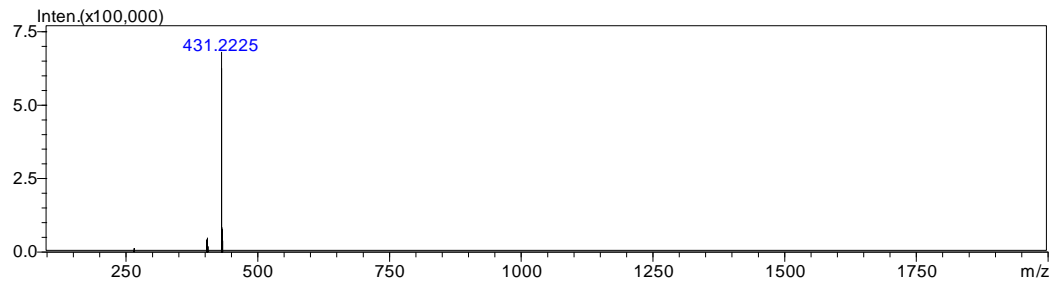
EN1



NL1



S3



# Mass Spectrum SmartFormula Report

## Analysis Info

Analysis Name D:\Data\Chemistry\2014 Sample\Feb 2014\CAI.d  
Method tune\_low\_pos\_200ul.m  
Sample Name CAI  
Comment PROF YAO SQ

Acquisition Date 2/12/2014 5:18:13 PM

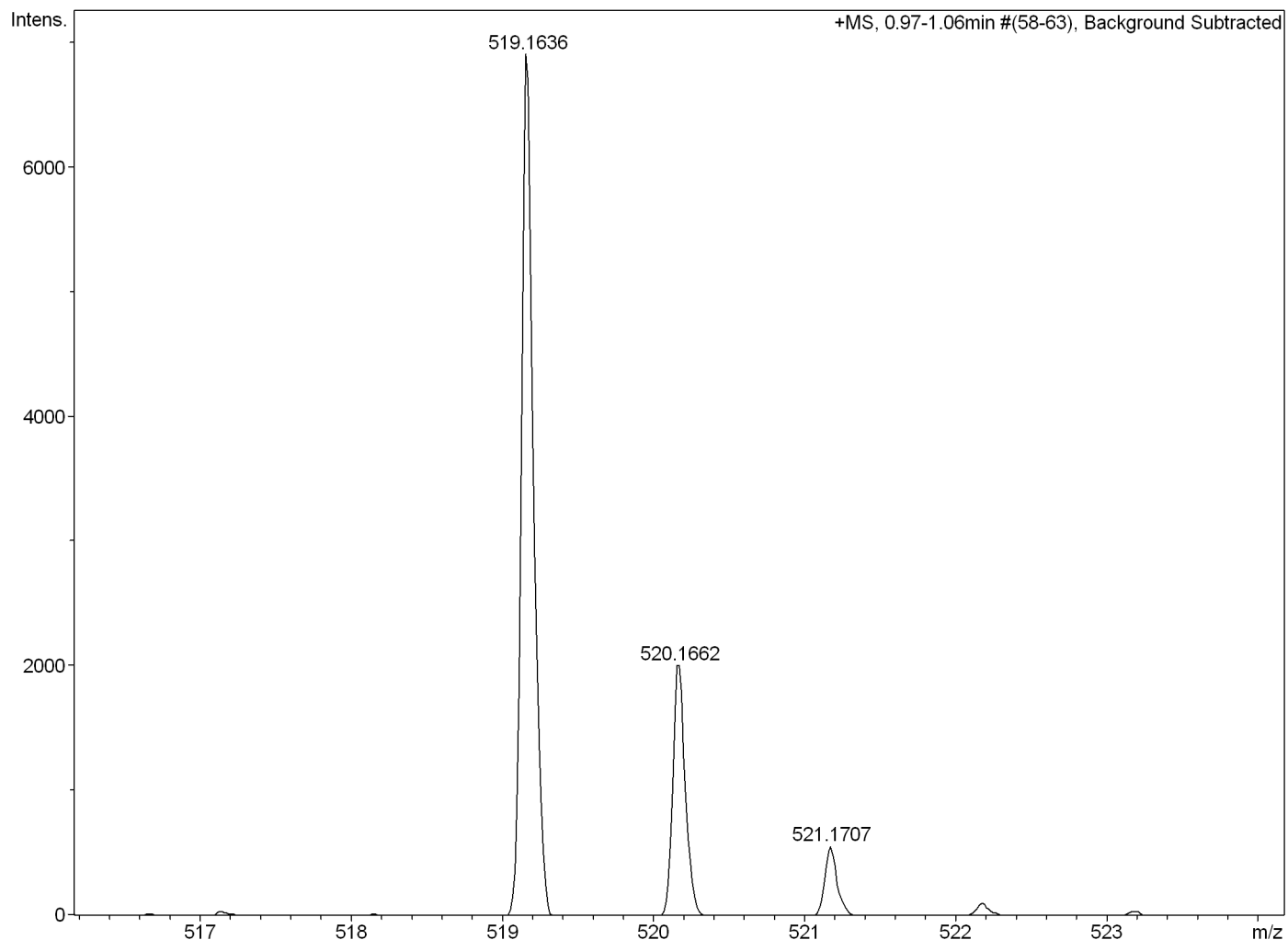
Operator default user

Instrument / Ser# micrOTOF-Q II 10269

## Acquisition Parameter

Source Type	ESI	Ion Polarity	Positive	Set Nebulizer	2.0 Bar
Focus	Not active	Set Capillary	4500 V	Set Dry Heater	200 °C
Scan Begin	50 m/z	Set End Plate Offset	-500 V	Set Dry Gas	5.0 l/min
Scan End	1500 m/z	Set Collision Cell RF	120.0 Vpp	Set Divert Valve	Waste

Meas. m/z	#	Formula	m/z	err [ppm]	rdb	e <sup>-</sup> Conf	N-Rule
519.1636	1	C 28 H 24 N 4 Na O 5	519.1639	0.6	18.5	even	ok



# Mass Spectrum SmartFormula Report

## Analysis Info

Analysis Name D:\Data\Chemistry\2014 Sample\Feb 2014\ENI.d  
Method tune\_low\_pos\_200ul.m  
Sample Name ENI  
Comment PROF YAO SQ

Acquisition Date 2/12/2014 5:40:35 PM

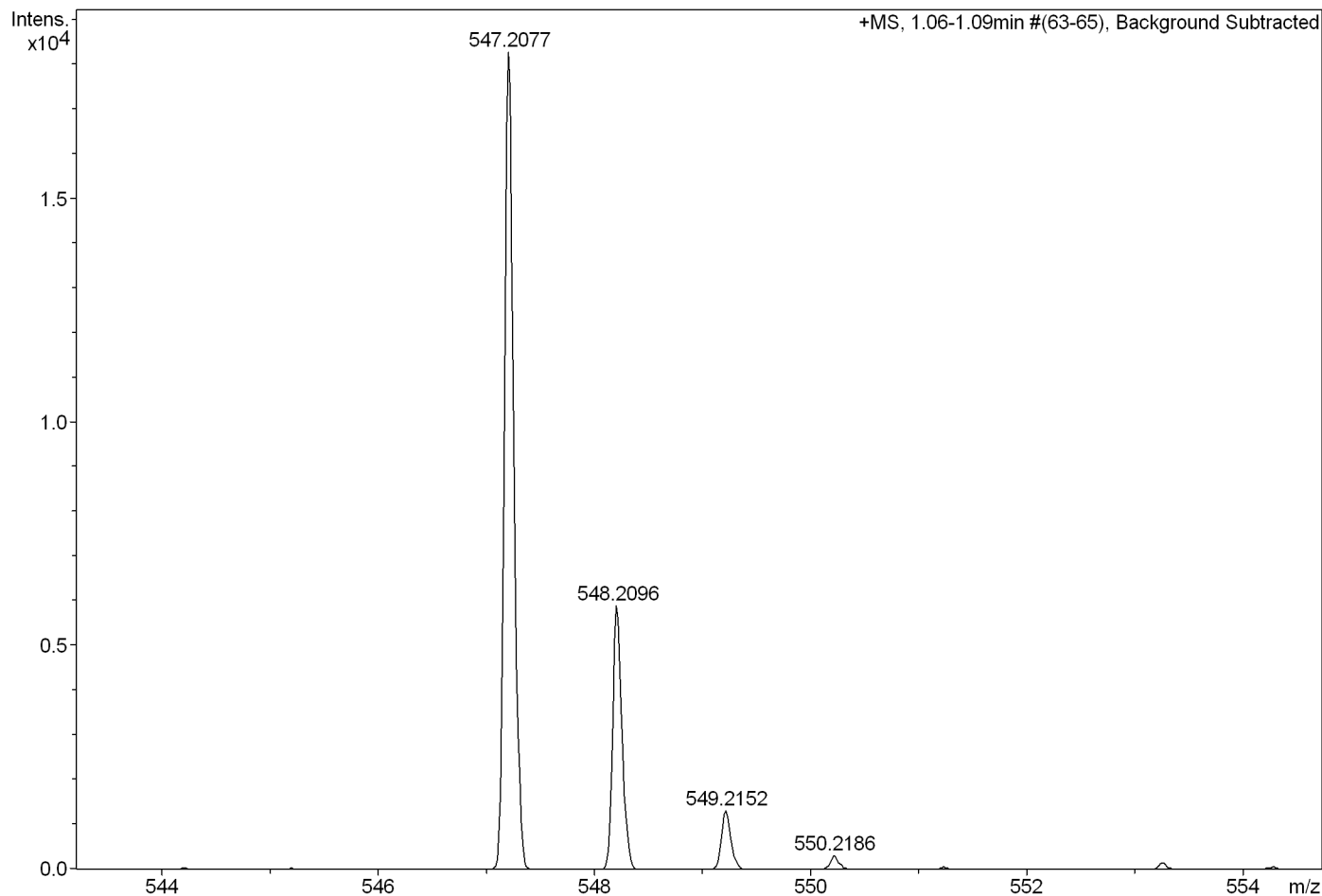
Operator default user

Instrument / Ser# micrOTOF-Q II 10269

## Acquisition Parameter

Source Type	ESI	Ion Polarity	Positive	Set Nebulizer	2.0 Bar
Focus	Not active	Set Capillary	4500 V	Set Dry Heater	200 °C
Scan Begin	50 m/z	Set End Plate Offset	-500 V	Set Dry Gas	5.0 l/min
Scan End	1500 m/z	Set Collision Cell RF	120.0 Vpp	Set Divert Valve	Waste

Meas. m/z	#	Formula	m/z	err [ppm]	rdb	e <sup>-</sup> Conf	N-Rule
547.2077	1	C 29 H 28 N 6 Na O 4	547.2064	-2.4	18.5	even	ok
	2	C 31 H 27 N 6 O 4	547.2088	2.0	21.5	even	ok
	3	C 34 H 28 N 4 Na O 2	547.2104	5.0	22.5	even	ok
	4	C 42 H 27 O	547.2056	-3.8	29.5	even	ok



# Mass Spectrum SmartFormula Report

## Analysis Info

Analysis Name D:\Data\Chemistry\2014 Sample\Feb 2014\FGI.d  
Method tune\_low\_pos\_200ul.m  
Sample Name FGI  
Comment PROF YAO SQ

Acquisition Date 2/12/2014 5:08:31 PM

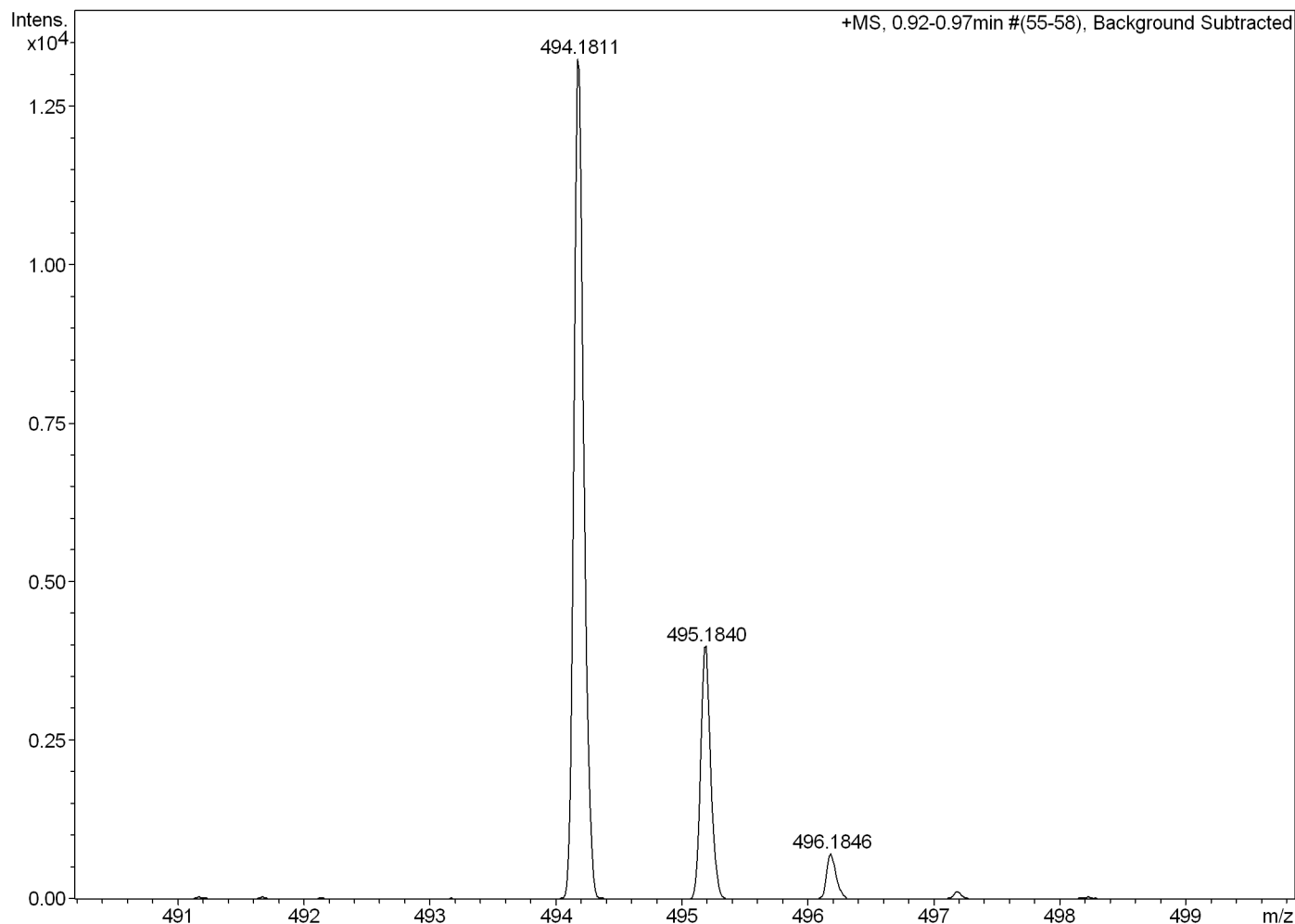
Operator default user

Instrument / Ser# micrOTOF-Q II 10269

## Acquisition Parameter

Source Type	ESI	Ion Polarity	Positive	Set Nebulizer	2.0 Bar
Focus	Not active	Set Capillary	4500 V	Set Dry Heater	200 °C
Scan Begin	50 m/z	Set End Plate Offset	-500 V	Set Dry Gas	5.0 l/min
Scan End	1500 m/z	Set Collision Cell RF	120.0 Vpp	Set Divert Valve	Waste

Meas. m/z	#	Formula	m/z	err [ppm]	rdb	e <sup>-</sup> Conf	N-Rule
494.1811	1	C 26 H 25 N 5 Na O 4	494.1799	-2.5	16.5	even	ok
	2	C 28 H 24 N 5 O 4	494.1823	2.4	19.5	even	ok



# Mass Spectrum SmartFormula Report

## Analysis Info

Analysis Name D:\Data\Chemistry\2014 Sample\Feb 2014\GWI.d  
Method tune\_low\_pos\_200ul.m  
Sample Name GWI  
Comment PROF YAO SQ

Acquisition Date 2/12/2014 5:01:53 PM

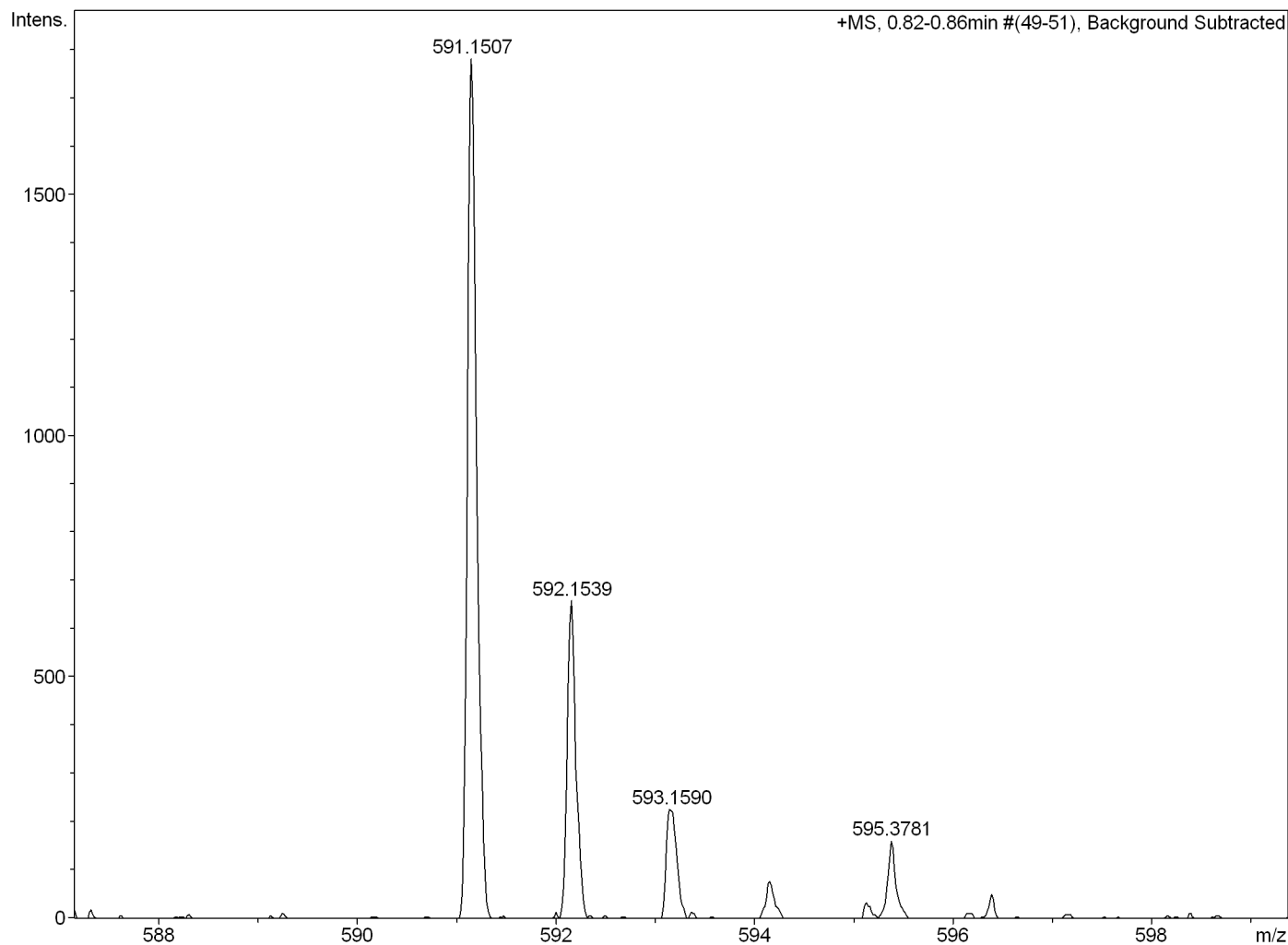
Operator default user

Instrument / Ser# micrOTOF-Q II 10269

## Acquisition Parameter

Source Type	ESI	Ion Polarity	Positive	Set Nebulizer	2.0 Bar
Focus	Not active	Set Capillary	4500 V	Set Dry Heater	200 °C
Scan Begin	50 m/z	Set End Plate Offset	-500 V	Set Dry Gas	5.0 l/min
Scan End	1500 m/z	Set Collision Cell RF	120.0 Vpp	Set Divert Valve	Waste

Meas. m/z	#	Formula	m/z	err [ppm]	rdb	e <sup>-</sup>	Conf	N-Rule
591.1507	1	C 28 H 27 F 4 N 4 O 2 S 2	591.1506	-0.2	15.5	even		ok



# Mass Spectrum SmartFormula Report

**Analysis Info**

Analysis Name D:\Data\Chemistry\2014 Sample\Feb 2014\ISI.d  
 Method tune\_low\_pos\_200ul.m  
 Sample Name ISI  
 Comment PROF YAO SQ

Acquisition Date 2/12/2014 5:33:58 PM

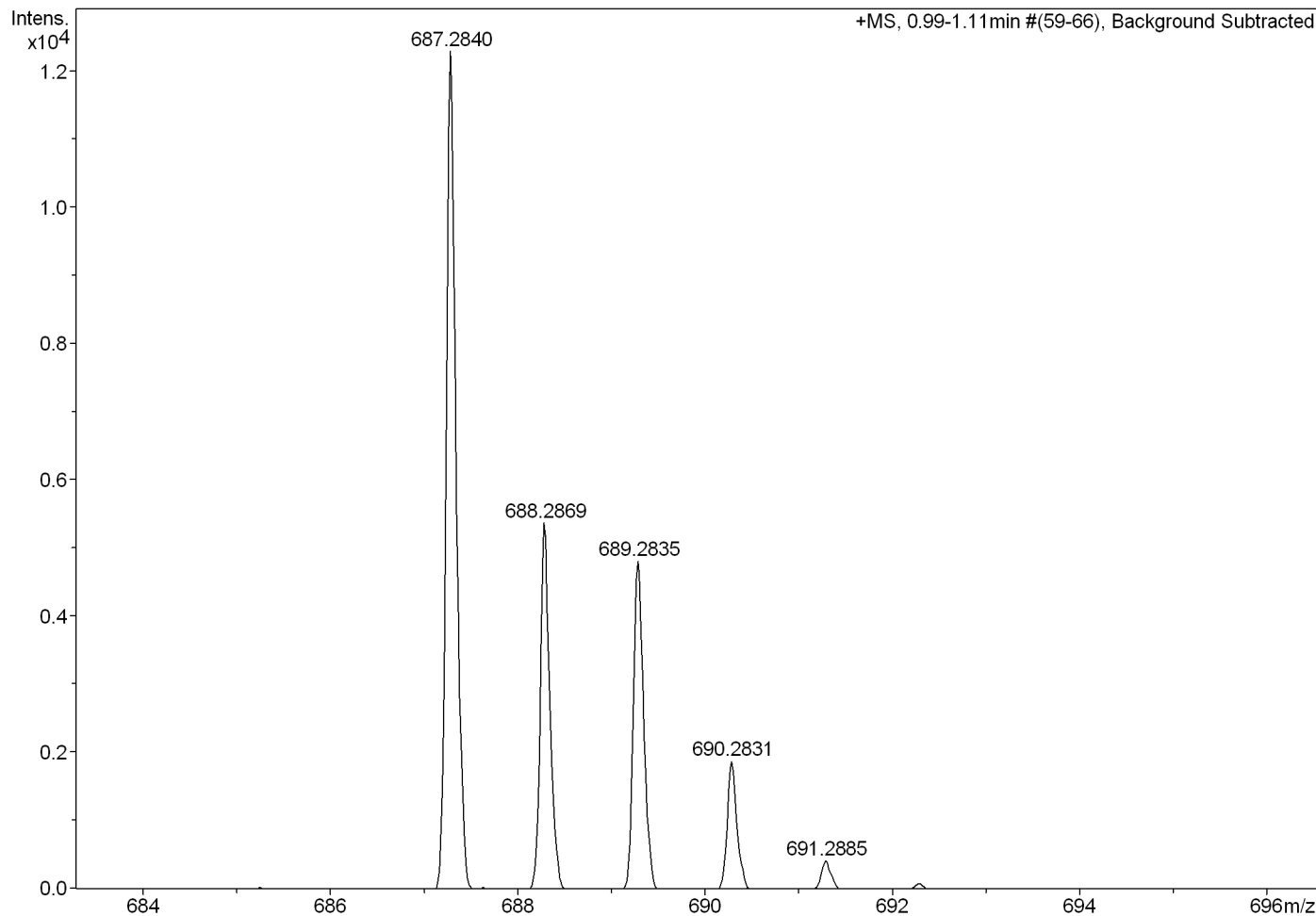
Operator default user

Instrument / Ser# micrOTOF-Q II 10269

**Acquisition Parameter**

Source Type	ESI	Ion Polarity	Positive	Set Nebulizer	2.0 Bar
Focus	Not active	Set Capillary	4500 V	Set Dry Heater	200 °C
Scan Begin	50 m/z	Set End Plate Offset	-500 V	Set Dry Gas	5.0 l/min
Scan End	1500 m/z	Set Collision Cell RF	120.0 Vpp	Set Divert Valve	Waste

Meas. m/z	#	Formula	m/z	err [ppm]	rdb	e <sup>-</sup>	Conf	N-Rule
687.2840	1	C 38 H 41 Cl N 6 Na O 3	687.2821	-2.8	20.5	even	ok	
	2	C 40 H 40 Cl N 6 O 3	687.2845	0.7	23.5	even	ok	
	3	C 43 H 41 Cl N 4 Na O	687.2861	3.1	24.5	even	ok	



# Mass Spectrum SmartFormula Report

## Analysis Info

Analysis Name D:\Data\Chemistry\2014 Sample\Feb 2014\NLI.d  
Method tune\_low\_pos\_200ul.m  
Sample Name NLI  
Comment PROF YAO SQ

Acquisition Date 2/12/2014 5:26:06 PM

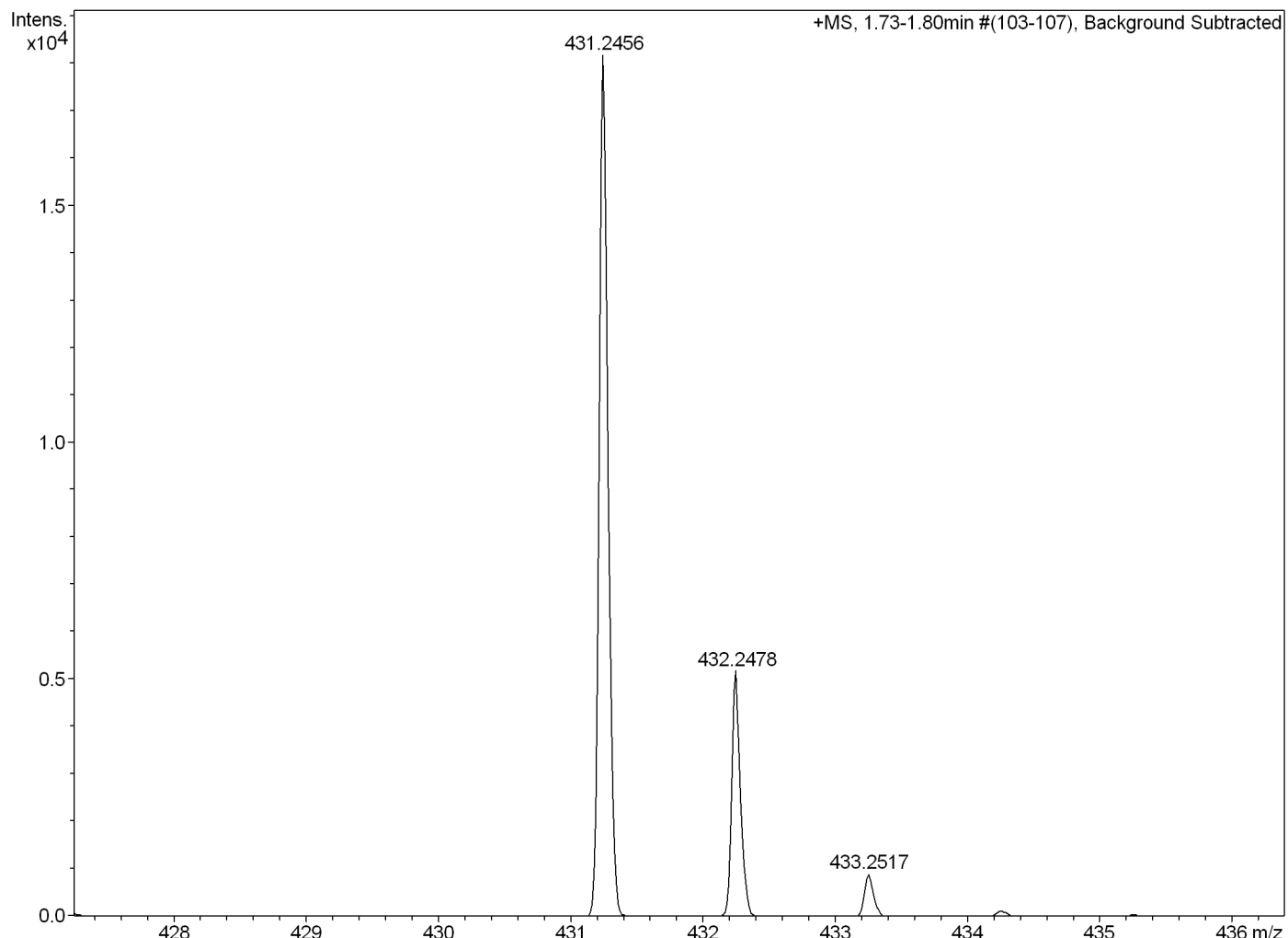
Operator default user

Instrument / Ser# micrOTOF-Q II 10269

## Acquisition Parameter

Source Type	ESI	Ion Polarity	Positive	Set Nebulizer	2.0 Bar
Focus	Not active	Set Capillary	4500 V	Set Dry Heater	200 °C
Scan Begin	50 m/z	Set End Plate Offset	-500 V	Set Dry Gas	5.0 l/min
Scan End	1500 m/z	Set Collision Cell RF	120.0 Vpp	Set Divert Valve	Waste

Meas. m/z	#	Formula	m/z	err [ppm]	rdb	e <sup>-</sup> Conf	N-Rule
431.2456	1	C 26 H 31 N 4 O 2	431.2442	-3.3	13.5	even	ok



# Mass Spectrum SmartFormula Report

## Analysis Info

Analysis Name D:\Data\Chemistry\2014 Sample\Feb 2014\XAI.d  
Method tune\_low\_pos\_200ul.m  
Sample Name XAI  
Comment PROF YAO SQ

Acquisition Date 2/12/2014 4:53:27 PM

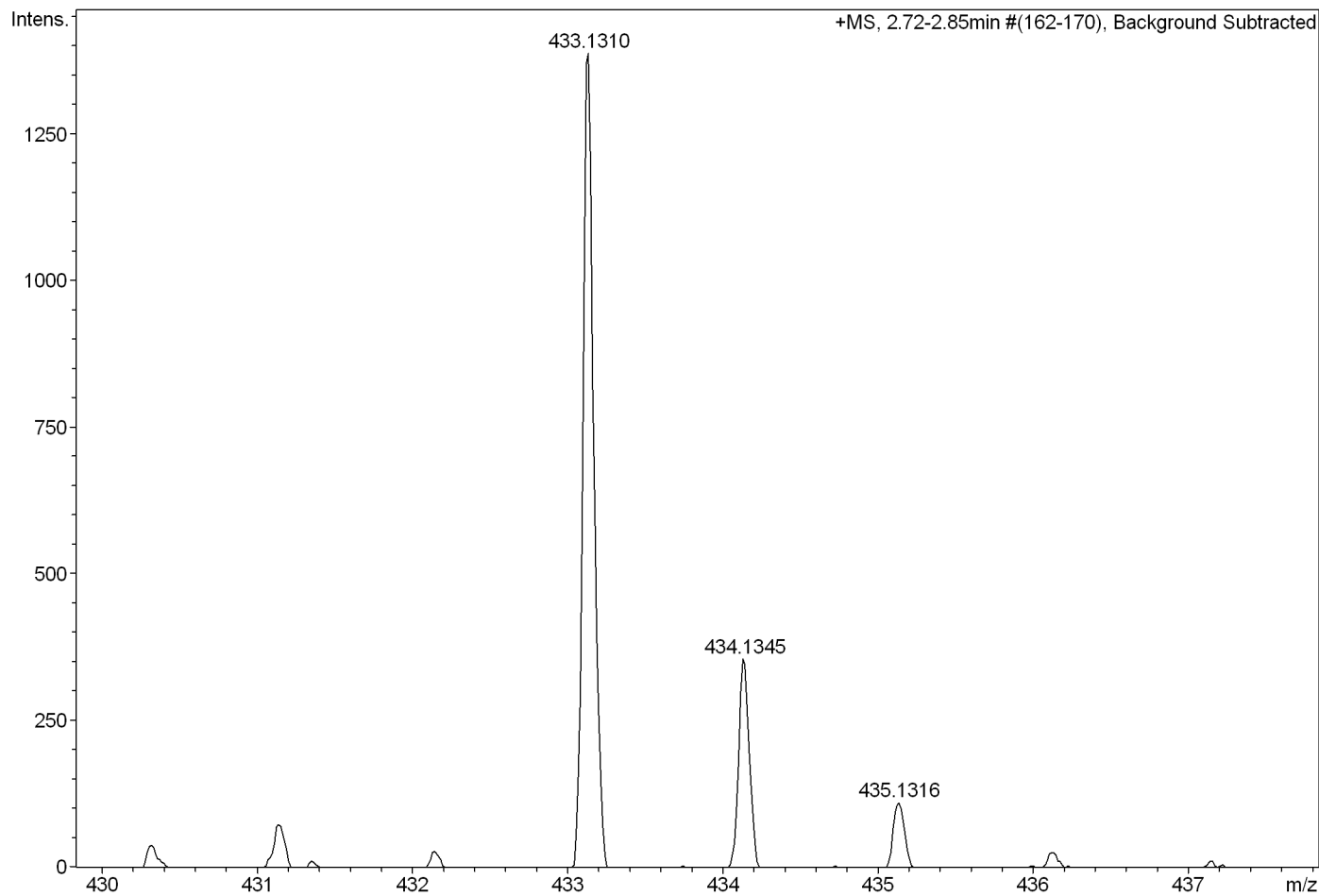
Operator default user

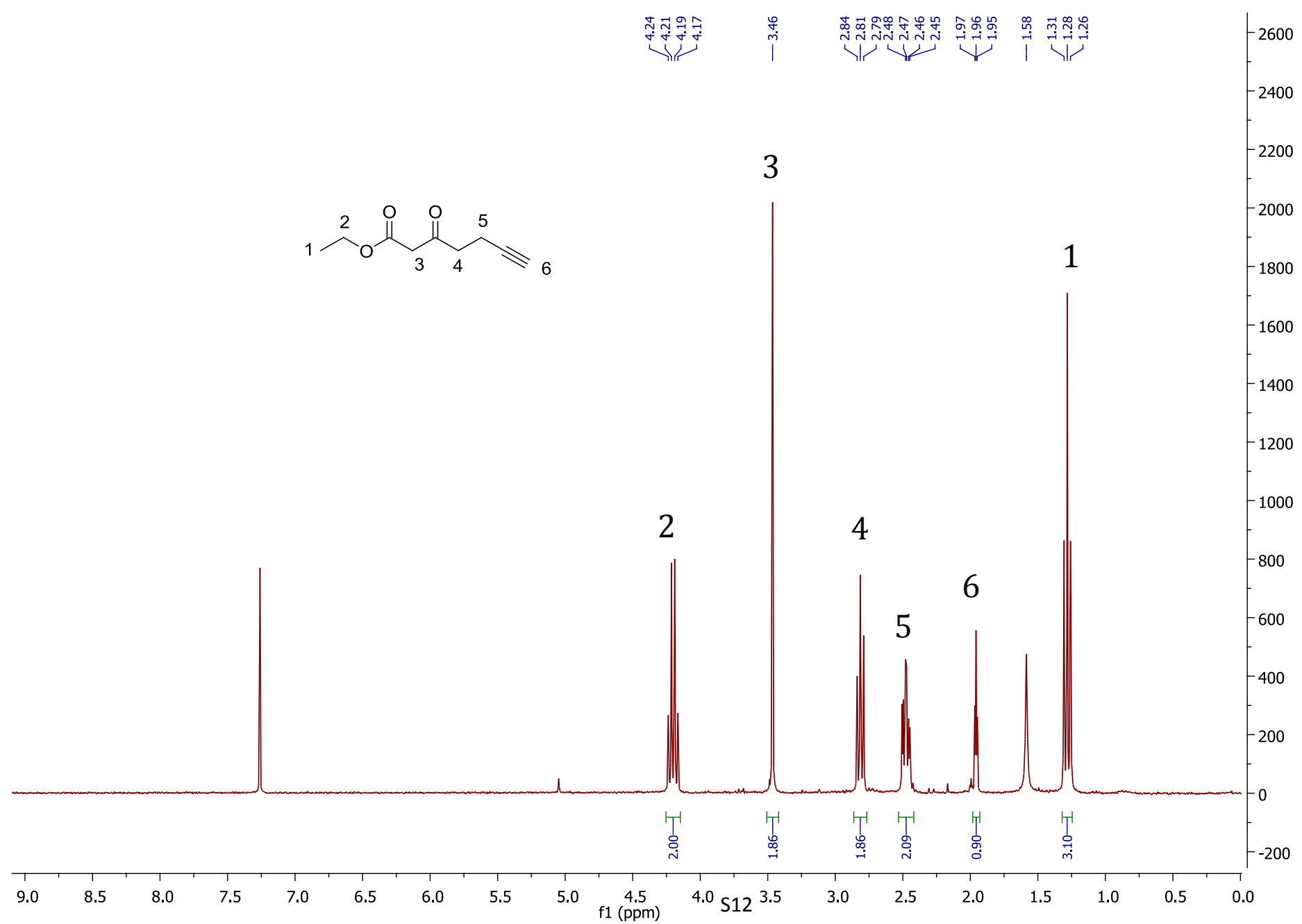
Instrument / Ser# micrOTOF-Q II 10269

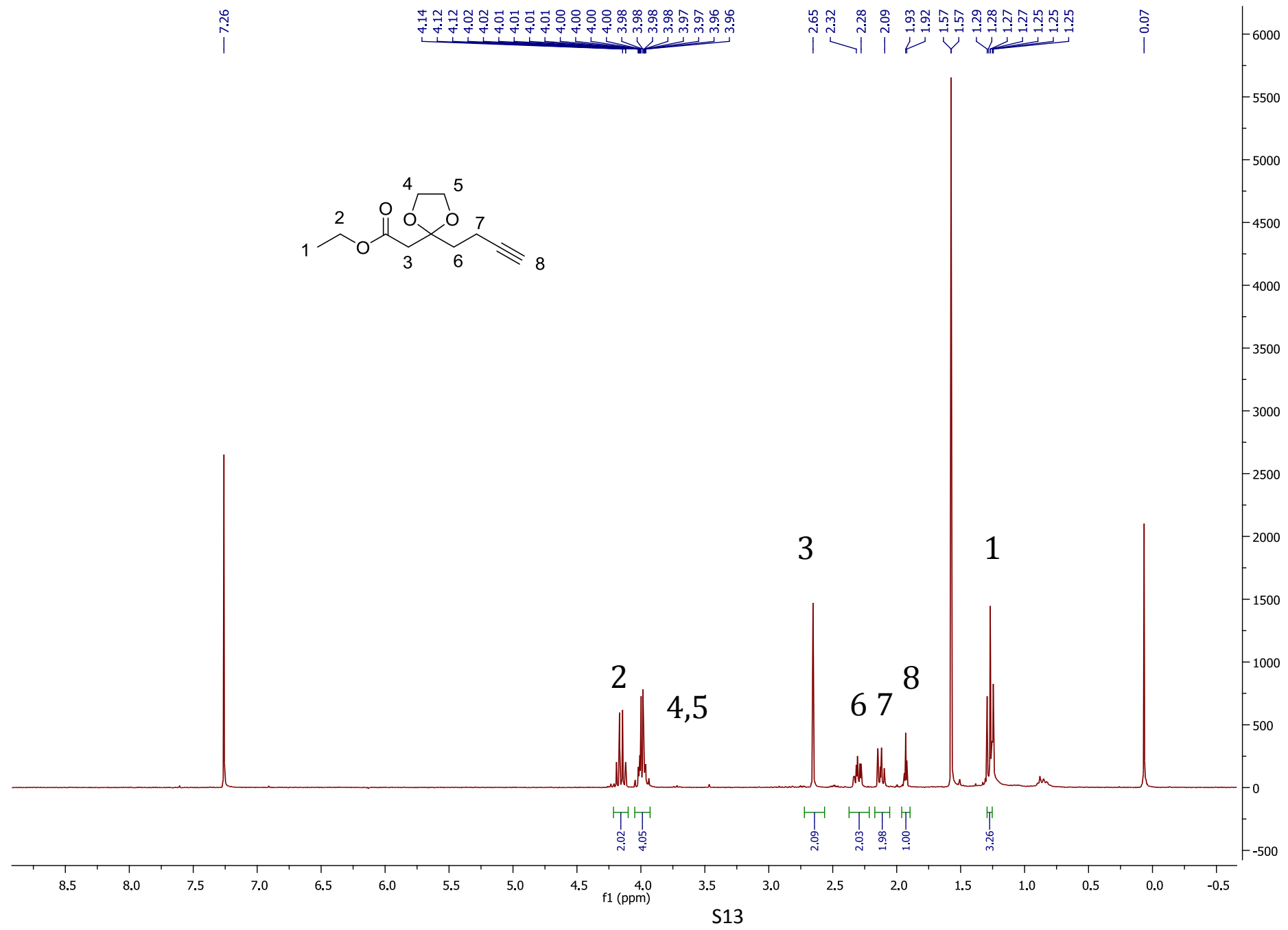
## Acquisition Parameter

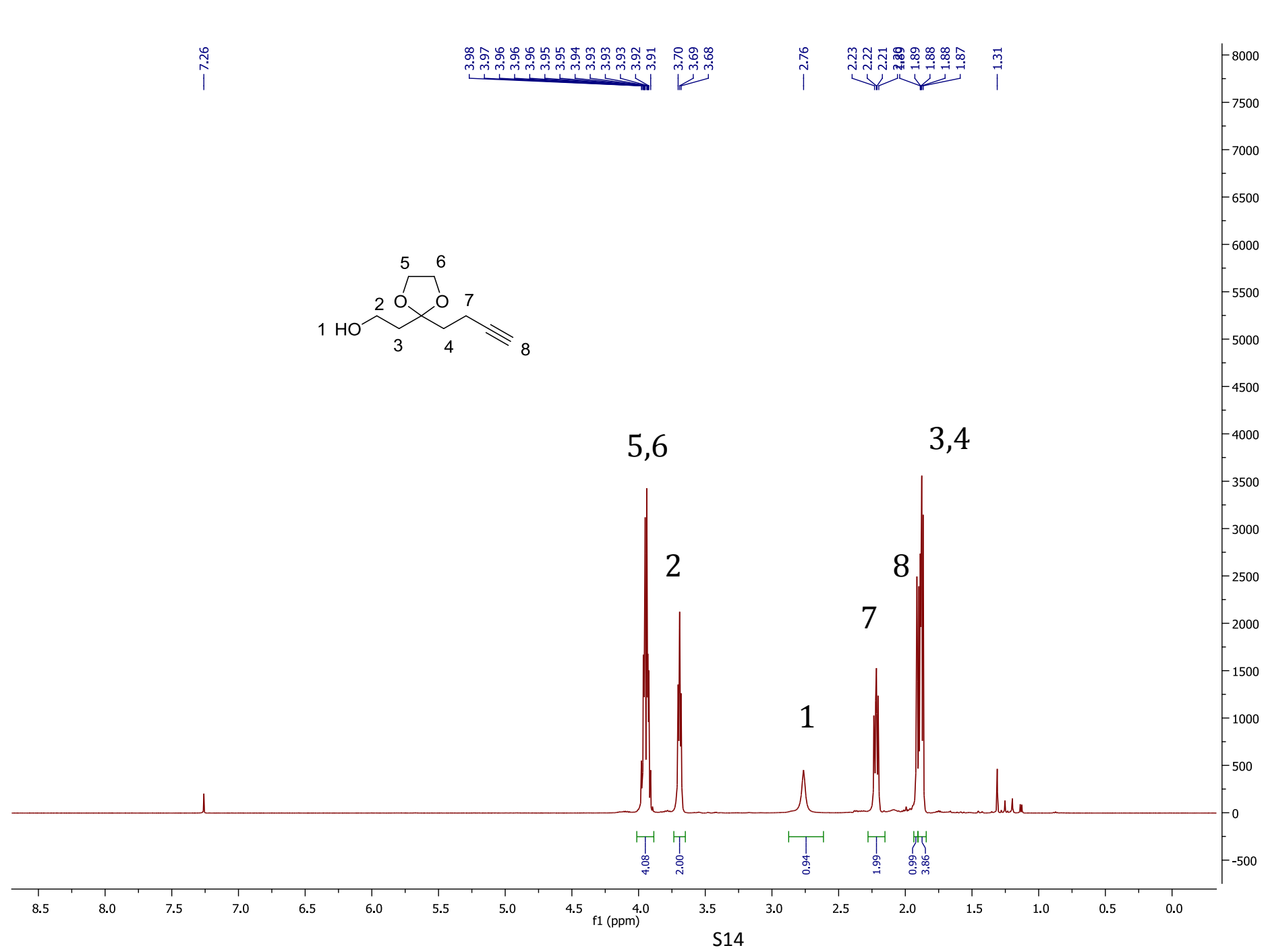
Source Type	ESI	Ion Polarity	Positive	Set Nebulizer	2.0 Bar
Focus	Not active	Set Capillary	4500 V	Set Dry Heater	200 °C
Scan Begin	50 m/z	Set End Plate Offset	-500 V	Set Dry Gas	5.0 l/min
Scan End	1500 m/z	Set Collision Cell RF	120.0 Vpp	Set Divert Valve	Waste

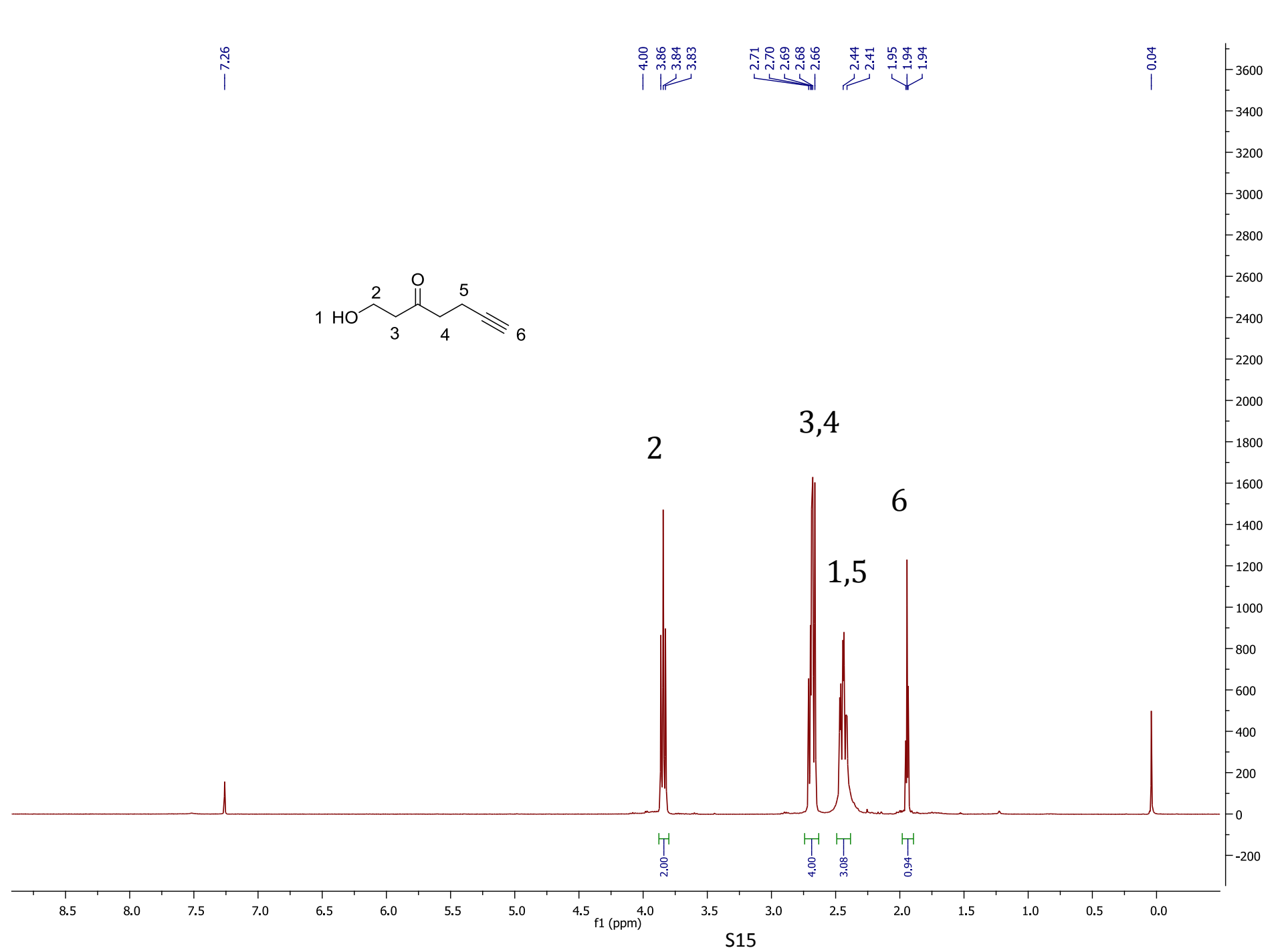
Meas. m/z	#	Formula	m/z	err [ppm]	rdb	e <sup>-</sup> Conf	N-Rule
433.1310	1	C 21 H 20 F 3 N 4 O S	433.1304	-1.4	12.5	even	ok
	2	C 24 H 19 F 2 N 4 S	433.1293	-4.0	16.5	even	ok
	3	C 26 H 21 F 2 N O S	433.1306	-0.9	16.0	odd	ok
	4	C 29 H 20 F N S	433.1295	-3.6	20.0	odd	ok



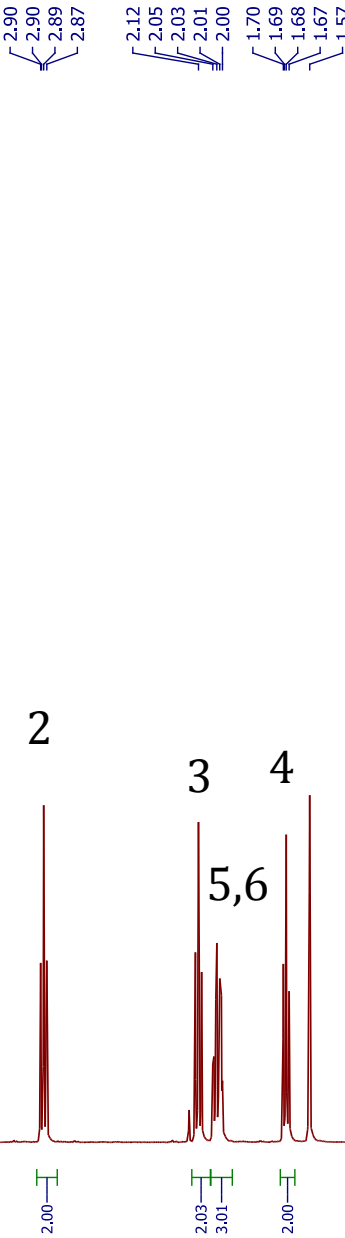
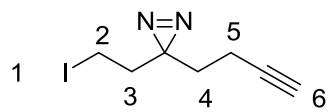








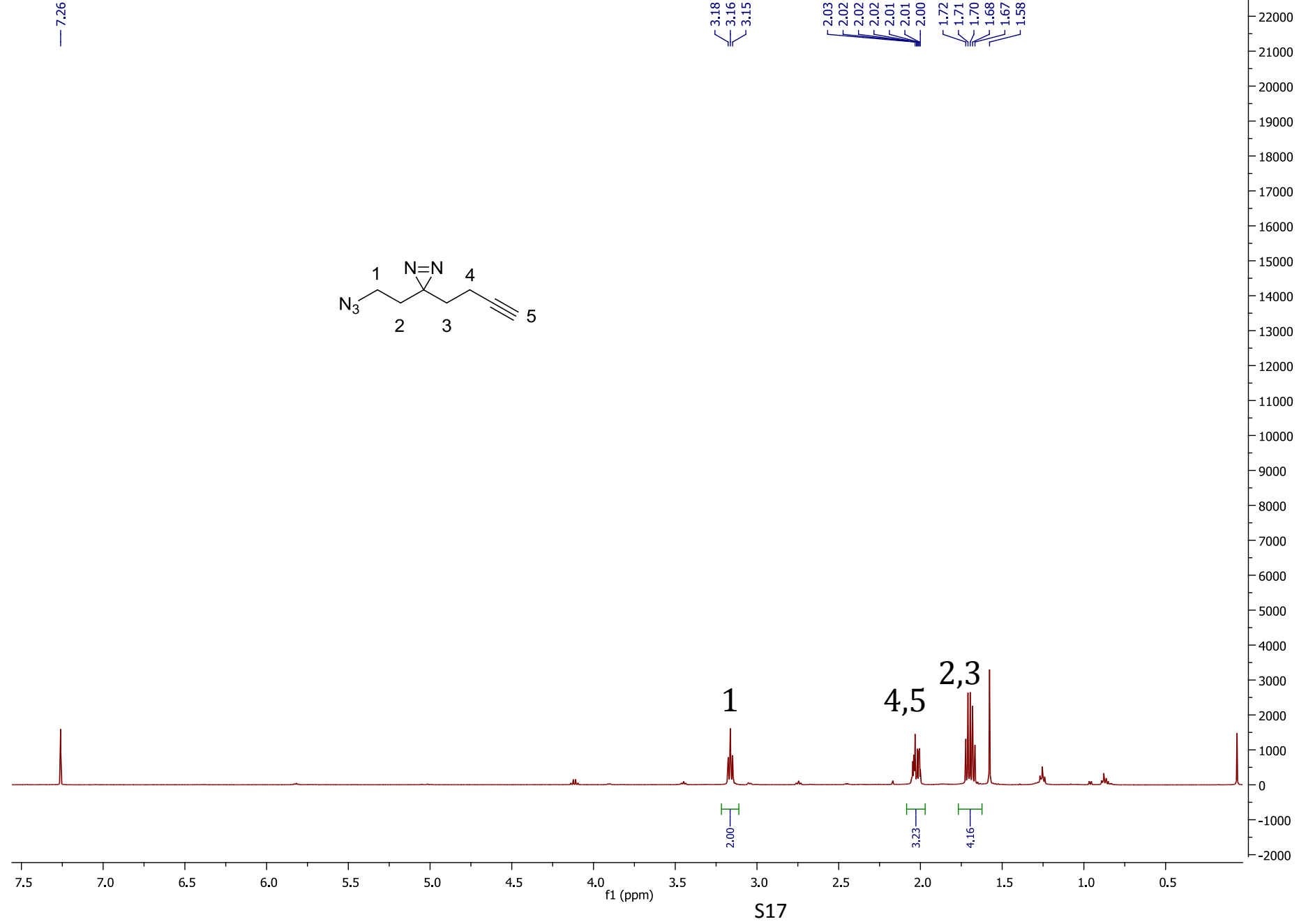
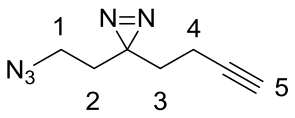
-7.26



f1 (ppm)

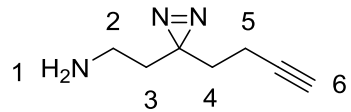
S16

— 7.26

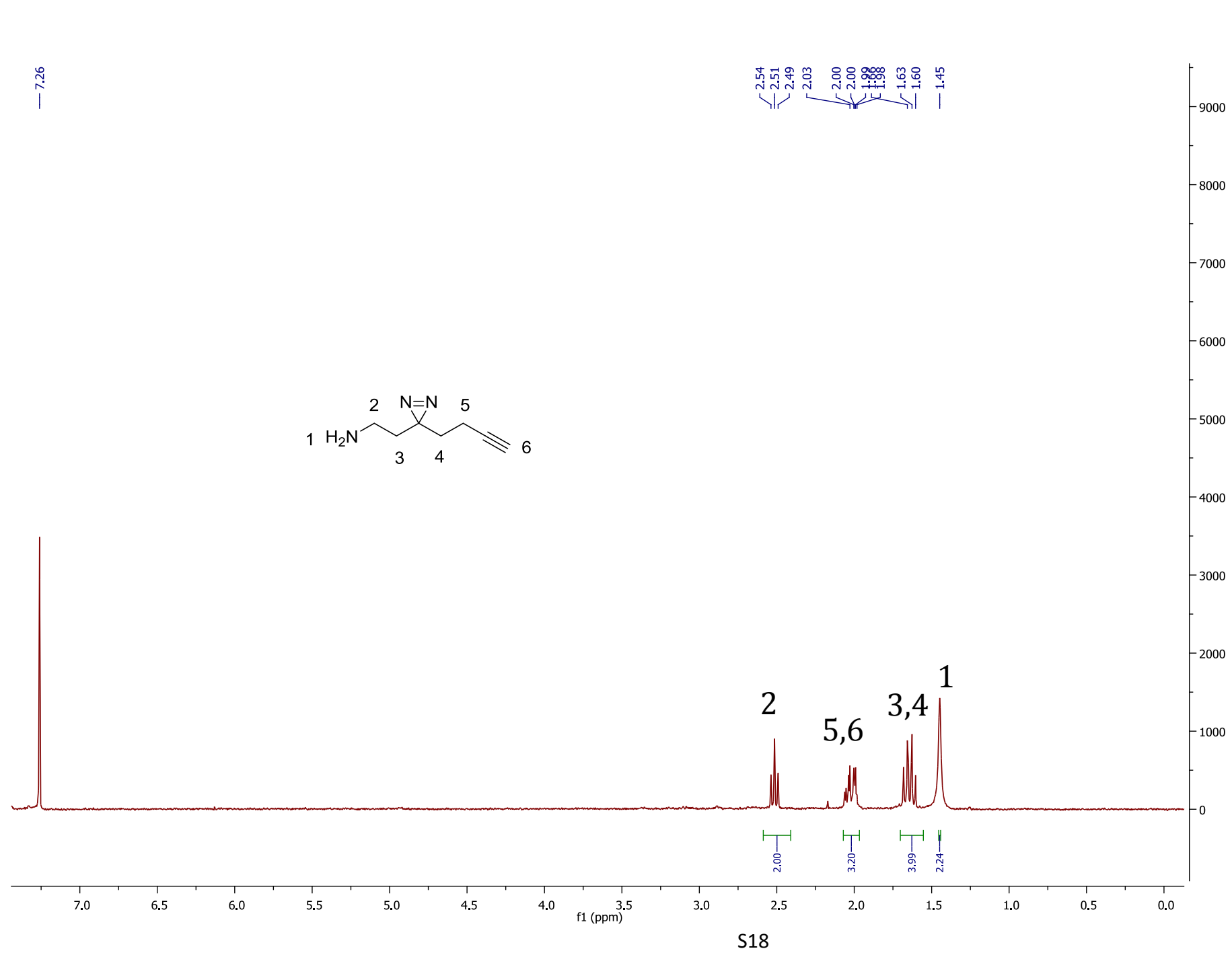


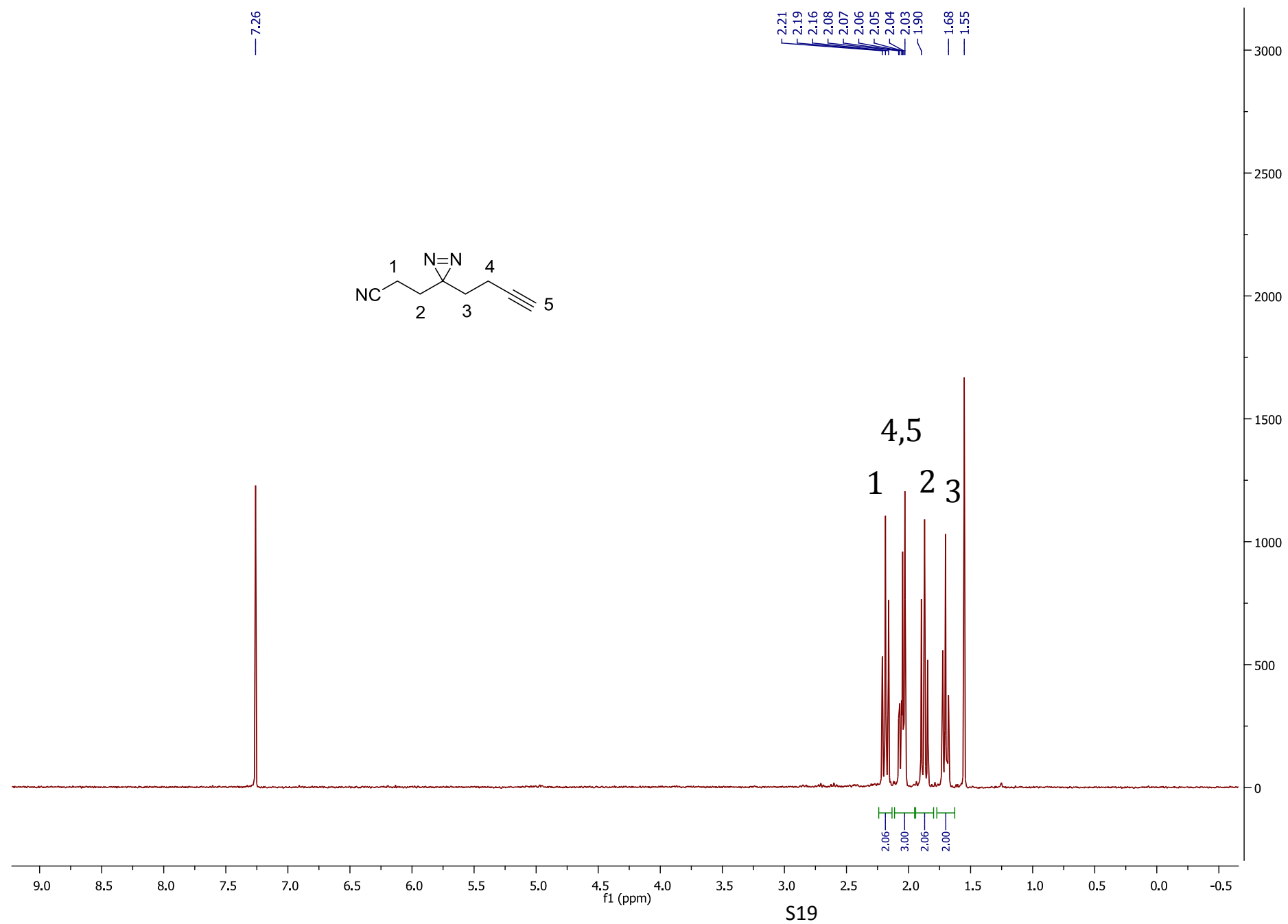
S17

— 7.26

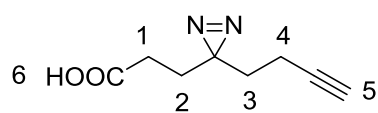


2.54  
2.51  
2.49  
2.03  
2.00  
1.99  
1.98  
1.63  
1.60  
1.45





— 7.26



2.20  
2.18  
2.17  
— 1.99  
— 1.80  
— 1.68  
— 1.66  
— 1.65

1 2 3

4,5

2.05  
3.02  
2.04  
2.00

S20

8.5 8.0 7.5 7.0 6.5 6.0 5.5 5.0 4.5 4.0 3.5 3.0 2.5 2.0 1.5 1.0 0.5 0.0

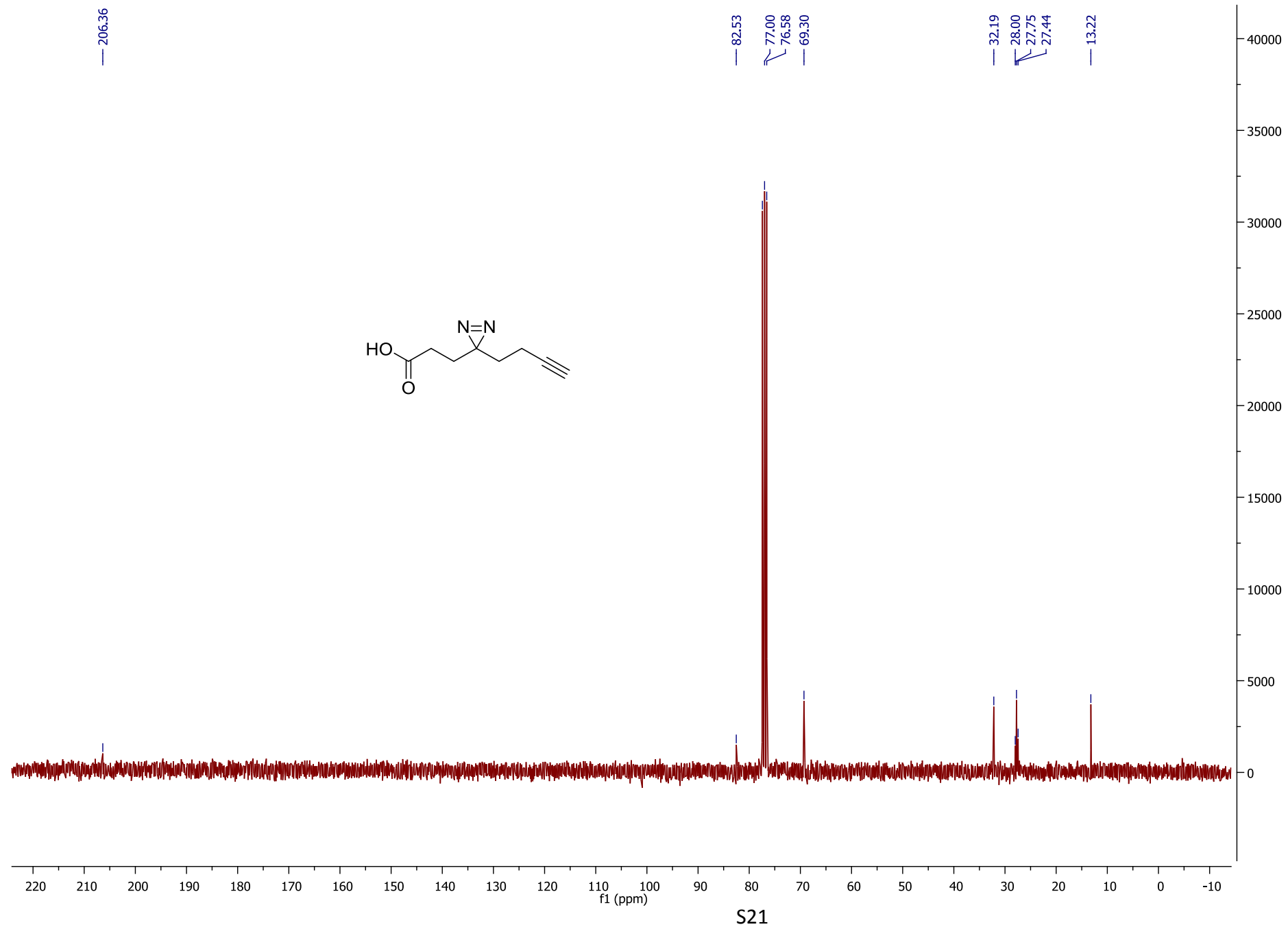
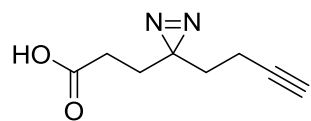
— 206.36

— 82.53

77.00  
76.58  
— 69.30

— 32.19  
28.00  
27.75  
— 27.44

— 13.22



7.74  
7.71  
7.69  
7.65  
7.63  
7.62

7.26  
7.22  
7.21  
7.19  
7.19

6.71  
6.69  
6.62

— 4.47

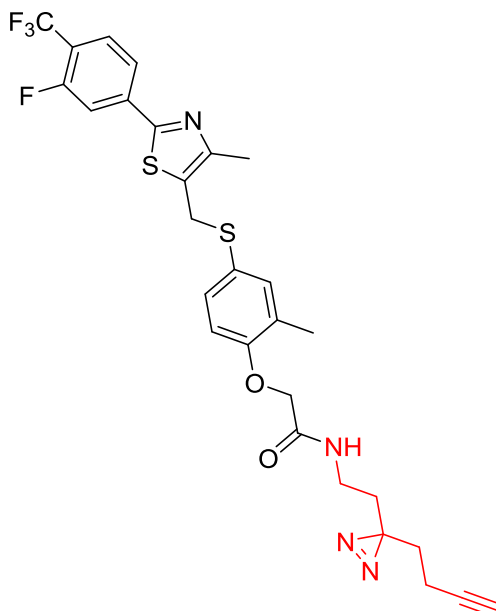
— 4.13

3.24  
3.23  
3.22  
3.20

— 2.29  
— 2.22

— 1.96

1.78  
1.77  
1.75  
1.66  
1.64  
1.63



1.93  
0.98

1.96

1.00  
1.02

2.03  
1.99

2.06

2.85  
3.13

3.06  
2.01  
2.29

